Department of Physics and Astronomy
University of Heidelberg

Master Thesis in Physics
submitted by

Caspar Groiseau

born in Berlin (Germany)

2017

Discrete-Time Quantum Walks in Momentum Space

This Master Thesis has been carried out by Caspar Groiseau at the
Institute for Theoretical Physics in Heidelberg
under the supervision of
PD Dr. Sandro Wimberger

Abstract

Quantum walks differ from their classical analogue in the fact that the state of the walker is in a superposition of positions. In our case, the walkers are atoms of a spinor Bose-Einstein condensate kicked by a periodic optical lattice. Such a configuration up can be described by the quantum kicked rotor model. We break the spatial-temporal symmetry by using a directed ratchet motion. The direction of the movement is determined by the sign of the kicking potential, which directly depends from the sign of the detuning. The standing-wave laser is tuned between two hyperfine levels of the ground state to create a difference in sign. Additionally, we consider the conditions for quantum resonance to be fulfilled, so that the free evolution of the atoms vanishes, and we only have changes in the momentum at discrete moments in time. The mixing of the internal states, ergo the coin toss, is in practice performed with microwaves. We investigate how the analytic theory of the temporal evolution of the quantum kicked rotor at quantum resonance can be transferred to two internal spin states that are mixed at each step.

Quantenirrfahrten unterscheiden sich von ihrem klassischen Analogon dadurch, dass der Läufer sich in einer Überlagerung aller Positionen befindet. In unserem Fall sind die Läufer Atome eines Spinor-Bose-Einstein Kondensates, welches periodisch von einem optischen Gitter gekickt wird. Für diese Konfiguration können wir das Modell des gekickten Rotors benutzen. Wir brechen die Symmetrie in Ort und Zeit durch Benutzung einer gerichteten Ratschen-Bewegung. Die Richtung der Bewegung ist durch das Vorzeichen der Kickpotenziales gegeben, welches direkt von der Verstimmung abhängt. Der Stehwellenlaser ist zwischen die beiden Hyperfeinzustände des Grundzustandes gestimmt, sodass die Vorzeichen für beide unterschiedlich sind. Zusätzlich nehmen wir an, dass die Voraussetzungen für Quantenresonanz erfüllt sind, sodass die freie Entwicklung der Atome verschwindet und wir nur zu diskreten Zeitpunkten Änderungen im Impuls haben. Das Mischen der internen Zustände, also der Münzwurf, wird in der Praxis mit Mikrowellen durchgeführt. Wir untersuchen wie die analytische Theorie der Zeitentwicklung des gekickten Rotors in Quantenresonanz auf zwei interne Spinzustände, die jeden Schritt gemischt werden, übertragen werden kann.

Contents

Introduction

Motivation

In the 1970s a paradigm shift announced itself, no longer were quantum mechanics 'merely' used to describe quantum systems encountered in nature but humanity started to design quantum systems to accomplish specific tasks. Today the resulting field of quantum information theory is blooming [1] with the more and more quantum technologies finding their way into concrete applications like quantum computation, quantum communication, quantum simulators and quantum cryptography.

Quantum walks (initially also referred to as quantum random walks) were conceived in 1993 by Aharonov, Davidovich and Zagury [2] are one of these new engineered quantum systems. As they are in short the quantum mechanical analogue to a classical random walk they are especially interesting for the field of quantum computation. The reason is that in classical computer science a lot of algorithms are based on random walks, everywhere were they are used there is the hope that a quantum walk could lead to speed ups in the computation time. An example for such problems are satisfiability problems and search of data banks which are solved by random walks over the graphs representing the problem. How fast the problem is solved depends on the hitting time, the time that it takes on average for the random walks to hit a certain subspace of the graph. It was shown that quantum walks have occasionally an exponentially shorter hitting time [3]. But quantum walks may be an even more powerful tool as recently it was shown by Childs that they are a primitive for universal quantum computation [4].

Since the discovery of quantum walks concrete realization were discussed for years. Recently the first actual implementations were achieved. Quantum walks were implemented with photons using a time-multiplexing technique [5] or with cold atoms in optical lattices [6] for example. In this thesis we want to investigate a new quantum walk scheme using the atom optics kicked rotor that was proposed by Summy and Wimberger [7] in which the walk in contrast to the earlier schemes with cold atoms did not take place in real space but rather in the reciprocal space. One of the main motivations for this new scheme is the fact that the atom optics kicked rotor is a well-studied and easy to implement system. and the two degrees of freedom needed for the walk are well separated.

The proposition is based on the δ-kicked rotor, a model that describes a particle that is periodically hit by δ-like pulses. The use of this system is also the reason why the walk takes place in momentum space as the natural description of the kicked rotor takes place in momentum space. Historically the kicked rotor was a paradigm of quantum chaos, the study of quantum system which classical analogue show chaotic dynamics. The classical kicked rotor is characterized by the chaotic Chirikov-Taylor or Standard map [8]. The quantum counterpart, the quantum kicked rotor knows two regimes that are vastly different from the classical dynamics: quantum resonance [9], where energy grows ballistically and dynamical localization [9], where its growth is stopped after a certain time called quantum break time. The first one is especially interesting for this thesis as it allows the implementation of directed matter wave currents, so-called quantum resonance ratchets.

As for all other quantum mechanical systems that are studied in experimental set ups this system does not constitute a closed system, lacking perfect isolation of the experiment will cause a coupling with the environment. The system is then said to be open. The system will develop decoherence, the loss of coherence, and the associated classical appearance. In our case spontaneous emission, the random relaxation of an excited atom is such an effect. Spontaneous emission causes the atom to change from the excited state to the ground state and to eject the corresponding energy as a photon in a random direction, thus leading to a counterbalancing and random change of the atomic momentum.

Outline

Chapter 1 gives a general introduction to the underlying theoretical and experimental preliminaries of this thesis. We review the concept of the atom optics kicked rotor and the needed derivatives of quantum resonance and quantum ratchets. And finally after having briefly given an overview of the field of quantum walks we present the new scheme for discrete-time quantum walks in momentum space of [7].

In Chapter 2 we present the numerical concepts that were used to implement the simulations of the system.

In Chapter 3 we start from the proposed experimental implementation of the quantum walk scheme and try to get to the theoretical result. We give the quantum optical description of the system and derived the effective kick dynamics.

In Chapter 4 investigate the theoretical model of the quantum walk. We derive the final momentum distribution and observe its dependence on its two parameters the kick strength and the kick number.

In Chapter 5 we regard the system to be open and interact with an environment of radiation modes leading to the appearance of spontaneous emission. We set up a master equation for the system and study how decoherence affects the walk.

1. Preliminaries

In this chapter we will introduce the background concepts that are required in this thesis. We start by introducing the experimental implementation and theoretical description of the atom optics kicked rotor. Furthermore we give a brief introduction to quantum walks and describe how those concepts are combined for the realization of discrete-time quantum walks in momentum space.

1.1. Atom Optics Kicked Rotor

1.1.1. Experimental Implementation

The δ-kicked rotor model has the advantage of not just being a toy model but being accessible to experimentally. The first one to realize it with cold atoms was the Raizen group in Austin, Texas [10]. Modern experiments use Bose-Einstein condensates [11, 12]. Here a short summary of the experimental implementation of the atom optics kicked rotor:

The basis for the atom optics kicked rotor is a set of alkali atoms, which are cooled by various sophisticated quantum optical techniques below the critical temperature of Bose-Einstein condensate formation. It is assumed that the set is diluted enough that interaction between the atoms can be neglected. After having been sufficiently cooled the atoms are released from the trap. The standing wave is created by shining a laser on a mirror so that the outgoing counter-propagating beam aligns with the incoming. The periodic pulsing is induced with an acousto-optic modulator with which one can control the intensity of the passing beam. After the kick sequence is finished the atoms are imaged via time-of-flight imaging. For this the atoms are allowed to expand freely for a short time in the order of milliseconds and are then targeted with near resonant light. The resulting fluorescence of the atoms is captured with a charge-coupled device.

Of course in the real world it is impossible to implement δ-like kicks but experimentalists have reported that with $100\text{ns} - 1\mu\text{s}$ pulse lengths the approximation is quite good [13].

1.1.2. Theoretical Description

The experimental set up described in the previous section leads to an effective Hamiltonian of the following sort [10]:

$$H_{\text{exp}} = \frac{p^2}{2M} - V_0 \cos(2k_L x) \sum_{j \in \mathbb{Z}} \delta(t - j\tau) \tag{1.1}$$

where p is the momentum, x the position, M the mass of the atom, k_L the wave vector of the standing-wave laser, τ the period of the kick pulses and V_0 the potential depth.

Generally the Hamiltonian is manipulated in 'natural units' rather than laboratory units due to the fact that it facilitates the notation in analytics and simulations. The units are rescaled in the following manner:

$$E \rightarrow \frac{E}{8 \frac{\hbar^2 k_L^2}{2M}}$$
$$p \rightarrow \frac{p}{2\hbar k_L} \tag{1.2}$$
$$x \rightarrow 2k_L x$$
$$\tau \rightarrow 2\pi \frac{\tau}{T_{\frac{1}{2}}}$$

where $T_{\frac{1}{2}}$ is the half Talbot-time

$$T_{\frac{1}{2}} = \frac{2\pi M}{\hbar G^2}. \tag{1.3}$$

G is the grating

$$G = 2k_L. \tag{1.4}$$

We end up with the following rescaled Hamiltonian:

$$H(t) = \frac{\hat{p}^2}{2} + k \cos \hat{x} \sum_{j \in \mathbb{Z}} \delta(t - j\tau) \tag{1.5}$$

where k is the kick strength

$$k = \frac{V_0 \tau_p}{\hbar} \tag{1.6}$$

and τ_p the duration of the kick pulse.

The time evolution operator describing the dynamics of the kicked atom, after a kick until the next one, is established by the unitary one-cycle Floquet operator [14]

$$\hat{U} = e^{-i \int_t^{t+\tau} H(t')dt'} = e^{-ik \cos \hat{x}} e^{-\frac{i}{2}\tau \hat{p}^2}, \tag{1.7}$$

where we additionally put $\hbar = 1$. The two parts of our Floquet operator, the kick part and the free evolution part factorize. The idea here is that while the kick happens, because of the δ-function, the action of the free evolution is vanishingly small compared to the kick so that it can be ignored.

As mentioned earlier the atom optics kicked rotor was thought of as an experimental implementation of the quantum kicked rotor. While the quantum kicked rotor describes particles moving on a circle the atoms in the atom optics kicked rotor move on a line. One can be mapped onto the other by exploiting the periodicity of the potential and introducing the concept of β-rotors.

This Hamiltonian (1.5) is 2π-periodic so we impose the spatial boundary conditions

$$\theta = x \quad \mathrm{mod}\ (2\pi) \tag{1.8}$$

so that $\hat{\theta}$ becomes our new angle operator.

Since we have a periodic potential, the Bloch theorem states that there is a basis of solutions to the stationary Schrödinger equation with the following form:

$$\psi(x) = e^{i\beta x}\psi_\beta(x) \tag{1.9}$$

where $\psi_\beta(x)$ is 2π-periodic

$$\psi_\beta(x + 2\pi) = \psi_\beta(x). \tag{1.10}$$

The periodic boundary conditions make it so that there only transitions between integer multiples n of momentum. Thus we separate the momentum into an integer part n and a conserved non-integer part $\beta \in [0; 1)$, that is called quasimomentum.

$$\hat{p} = \hat{n} + \beta \tag{1.11}$$

β is conserved because transitions between states that are not different by an integer in momentum are forbidden. The n are the eigenvalues of the angular momentum operator

$$\hat{n} = -i\frac{\partial}{\partial\theta} \tag{1.12}$$

The general solution of the Schrödinger equation $\psi(x)$ can be written as a superposition of Bloch waves $e^{i\beta x}\psi_\beta(x)$

$$\psi(x) = \int\limits_0^1 d\beta \rho_\beta e^{i\beta x}\psi_\beta(x). \tag{1.13}$$

Here ρ_β is the distribution of quasimomenta.

If the initial state of the atom is given by a plane wave with a discrete momentum

$$p_0 = n_0 + \beta_0 \tag{1.14}$$

the Bloch wave describing the system is:

$$\psi_\beta(\theta) = \langle \theta | \psi_\beta \rangle = \frac{1}{\sqrt{2\pi}} e^{in_0\theta} \tag{1.15}$$

$$\rho_\beta = \delta(\beta - \beta_0) \tag{1.16}$$

The time evolution of a β-rotor is described by the this new Floquet operator where we substituted the old variables by the new ones

$$\hat{U}_\beta = e^{-ik\cos\hat{\theta}} e^{-\frac{i}{2}\tau(\hat{n}+\beta)^2}. \tag{1.17}$$

1.1.3. Quantum Resonance

Quantum resonance [9] is an effect specific to the quantum regime and cannot be observed in the classical regime. For the main resonances the first part of the Floquet operator, the one associated to the free evolution, is equal to unity, so that we get a phase revival of the wave function in momentum space. The term 'main' is there to discern from so-called higher quantum resonances where powers of the free evolution term are equal to unity. The consequence of this is that the atoms directly after a kick and just before the next are in the same state. In this case there is no difference between T kicks of strength k and a kick of strength Tk.

$$\hat{U}_\beta = e^{-i\frac{\tau}{2}(\hat{n}^2+2\hat{n}\beta+\beta^2)} = 1 \tag{1.18}$$

Here the last part can be ignored as it has no n-dependency and will just produce a constant global phase that will cancel out when calculating expectation values. Hence we only have to satisfy

$$e^{-i\frac{\tau}{2}(\hat{n}^2+2\hat{n}\beta)} = 1 \tag{1.19}$$

which is the case for the following specific τ-β couples:

$$\tau = 2\pi l, \qquad\qquad\qquad l \in \mathbb{N} \tag{1.20}$$

$$\beta = \frac{1}{2} + \frac{i}{l} \mod (1), \qquad\qquad i = 0, 1, ..., l-1 \tag{1.21}$$

In this thesis we will consider $\tau = 4\pi$ and $\beta = 0$, which corresponds to a kick period that equals the Talbot time.

In quantum resonance the absorption of energy by the δ-kicked atoms from the kicking field is maximal. In this regime energy grows quadratically in time. This is in contrast to the linear energy growth for the classical kicked rotor.

$$E(T) = \langle \psi(T)| -\frac{1}{2}\frac{\partial^2}{\partial \theta^2}|\psi(T)\rangle \tag{1.22}$$

$$= -\frac{1}{4\pi}\int_0^{2\pi} e^{in_0\theta}e^{iTk\cos\hat{\theta}}\frac{\partial^2}{\partial\theta^2}e^{-iTk\cos\hat{\theta}}e^{-in_0\theta} \tag{1.23}$$

$$= \frac{n_0^2}{2} + \frac{k^2T^2}{4} \tag{1.24}$$

The quadratic growth can be traced back to the linear spread of the wave function in momentum space as can be seen in figure.
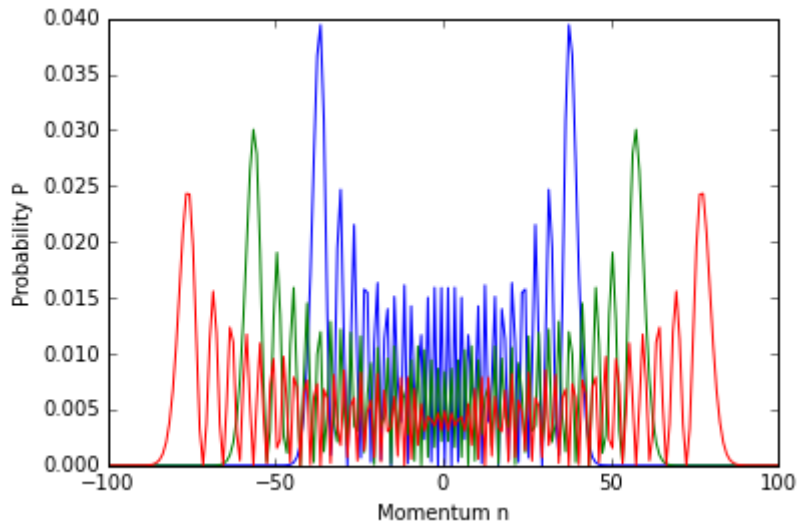
Figure 1.1.: Momentum distributions of the quantum kicked rotor with kick strength $k = 2$, an initial momentum of $n_0 = 0$ and kick numbers $T = 20$ (blue), $T = 30$ (green) and $T = 40$ (red).

A peculiarity of quantum resonance is that we can express the momentum distribution P analytically [18]

$$P(n; n_0, k, T) = J^2_{n-n_0}(kT), \tag{1.25}$$

where J is a Bessel functions of the first kind. A short summary of the most important aspects of Bessel functions of the first kind can be found in appendix A.

1.1.4. Quantum Ratchets

The name ratchet is derived from the Brownian or Feynman-Smoluchowski ratchet [19], a thought experiment conceived by Smoluchowski about a perpetuum mobile that at first glance due to its asymmetric structure seems to create a directed motion from an equilibrium posi-

tion, therefore violating the second law of thermodynamics.

Although this seeming contradiction could be resolved its interesting concept sparked the development of Brownian motors [20] and other systems that could gather useful work, for example a directed motion, from non-equilibrium.

A prime example for this kind of behaviour is the sawtooth ratchet [21]. In this system initially a wave function is localized in a well of an asymmetric sawtooth potential. The potential is hereinafter repeatedly switched on and off. When the potential is turned off the wave function diffuses. Ordinarily one will deal with stochastic forces or even opposing forces so the wave function might additionally shifted in a direction. After a while the potential is turned on again and now parts of the wave functions are trapped in different parts of the potential landscape. The form of the potential makes it more viable for the state to be in trapped on right side thus showing a net transport to the right.

When we are speaking about quantum ratchets we mean a ratchet effect in a quantum system. Cold atom ratchet are ultra-cold atoms whose initial momentum state is in a superposition state of multiple momentum classes. For an comprehensive review see [14]. Experimentally those systems are produced by coherently splitting a Bose-Einstein condensate with a momentum conserving Bragg pulse. The phase between the initial momentum classes can be customized by adding a free evolution after the Bragg pulse. Subsequently the system is kicked like the standard atom optics kicked rotor.

The most basic example for such a quantum ratchet state would be a superposition of two initial momentum classes :

$$|\psi_2(\phi)\rangle = \frac{1}{\sqrt{2}} \left(|n = 0\rangle + e^{i\phi}|n = 1\rangle \right) \tag{1.26}$$

Realize that unlike the just mentioned conventional sawtooth ratchet, here the ratchet is embodied by the quantum state and not the potential. We have a symmetric potential (1.5) and the symmetry is broken by the state itself.

Unlike the case of a momentum state without a superposition the ratchet system does not diffuse symmetrically around their initial momentum but rather the mean momentum increase linearly over time. The direction and speed of this change depends on the kick strength and the phase between initial momentum classes. The average momentum change per kicks for a state like (1.26) is

$$\langle p \rangle_{T+1} - \langle p \rangle_T = -\frac{k}{2} \sin \phi \tag{1.27}$$

The dependence of the initial state in momentum space in atomic diffraction in a standing wave was studied in [22, 23].
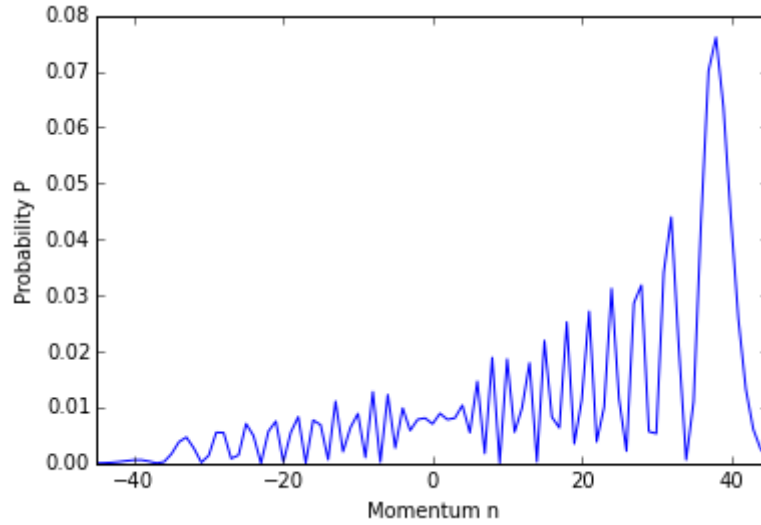
Figure 1.2.: Momentum distribution of the quantum ratchet state in (1.26) with a relative phase $\phi = -\frac{\pi}{2}$ after a kick sequence of strength $k = 2$ and length $T = 20$.

Of course one can also create more complex ratchet states with more momentum classes like

$$|\psi_3(\phi)\rangle = \frac{1}{\sqrt{3}} \left(e^{-i\phi}|n = -1\rangle + |n = 0\rangle + e^{i\phi}|n = 1\rangle \right). \tag{1.28}$$
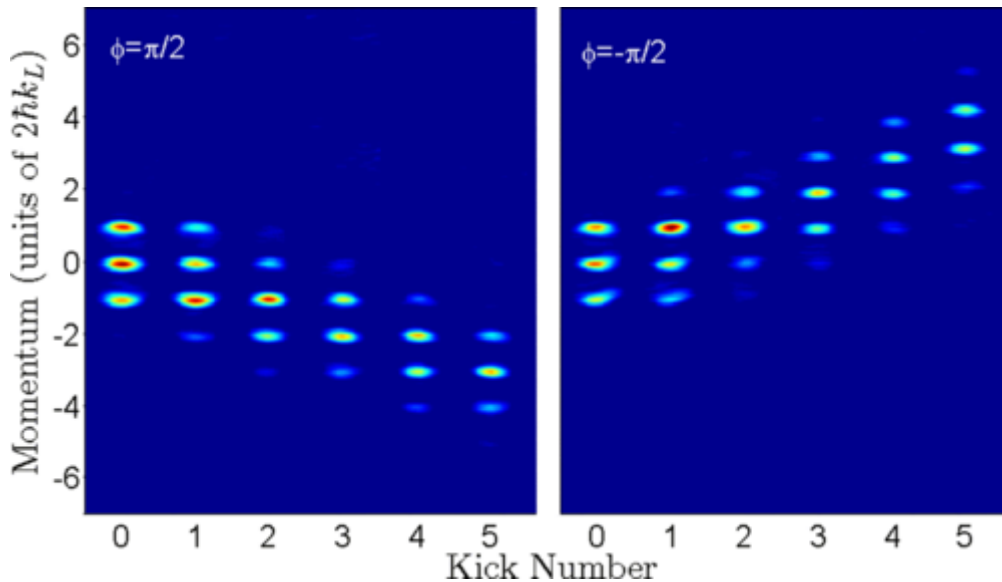
Figure 1.3.: Temporal evolution of a quantum ratchet with three initial momentum classes as described in (1.28) with exemplar influencing of the propagation direction by choice of the relative phase [7].

Although the average momentum change is directed in one direction still a not negligible amount of the momentum distribution diffuses in the other direction as can be perceived in.

Ratchets with more initial momentum classes have shown to be more resistant to this kind of dispersion [24]. This is especially true if the momentum classes are consecutive ones.

This behaviour can be explained qualitatively with the help of the following picture [25]. The effective force that the atom feels from the standing wave depends on the gradient of the standing wave.

$$F_{\text{eff}} = \left| \int_{-\pi}^{\pi} |\psi(x)|^2 \frac{dV(x)}{dx} dx \right| \tag{1.29}$$

The wave function is centred around the flank of the standing wave assuring a maximum of force. Now the gradient will vary over the area that the wave function extends therefore leading to varying effective force felt by the atoms. The more initial momentum classes the ratchet state has the narrower the wave function becomes, and ergo the larger the applied force becomes.
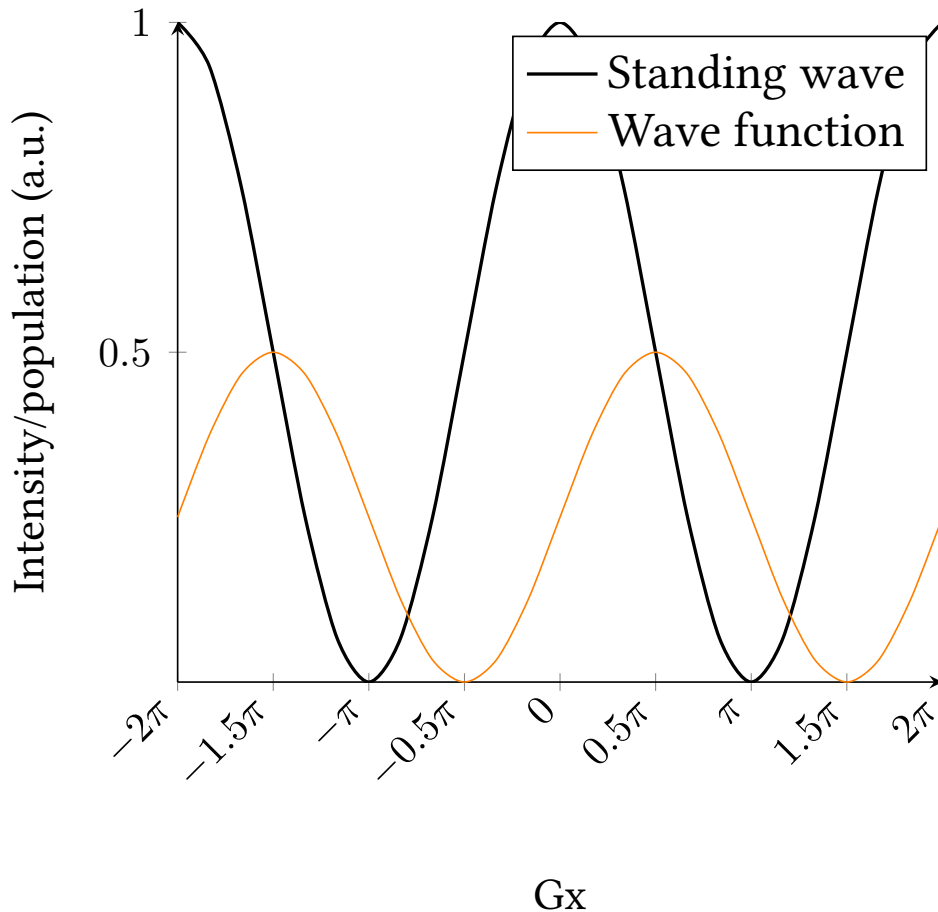
Figure 1.4.: Visualization of the functioning quantum ratchet mechanism. $G = 2k_L$ is the grating vector of the standing wave.

1.2. Quantum Walks

1.2.1. Basics

First of all there are two kinds of quantum walks: discrete-time and continuous ones. We will only be dealing with the former one. For a more thorough review of the concept of quantum walks we refer to [26].

Quantum walks are the quantum-mechanical analogue of classical random walks. Classically the walker at each step of the walk flips a coin and proceeds to take a step to the right or to the left depending on the outcome of the throw. After a certain number of steps the walker has a final position which distribution trends towards a Gaussian distribution if this procedure is repeated a great number of times. Now for a quantum walk next to the external degree of freedom corresponding to the position of the walker, the walker also possesses an internal one for example a spin. The walk consists of the application of two operators: a translation operator and a coin operator. The translation operator is spin-sensitive and will depend on the orientation in its internal degree of freedom move the walker one step to the left or to the right

$$T = \sum_i |\downarrow\rangle\langle\downarrow|\otimes|i-1\rangle\langle i| + |\uparrow\rangle\langle\uparrow|\otimes|i+1\rangle\langle i|. \tag{1.30}$$

It is clear that if the walker is in a state of superposition in its internal degree of freedom this superposition is transferred to its external degree of freedom. The coin operator as the name suggests, replaces the classical coin and effectively represents a rotation of the internal degree of freedom to recreate the superposition in it. The Hadamard gate would be a prominent example for such a balanced coin:

$$C = \frac{1}{\sqrt{2}} \begin{pmatrix} 1 & 1 \\ 1 & -1 \end{pmatrix} \tag{1.31}$$

The final result of repeatedly applying those two is that the walker is in a superposition of all possible positions.

Classical Random Walk   Quantum Walk
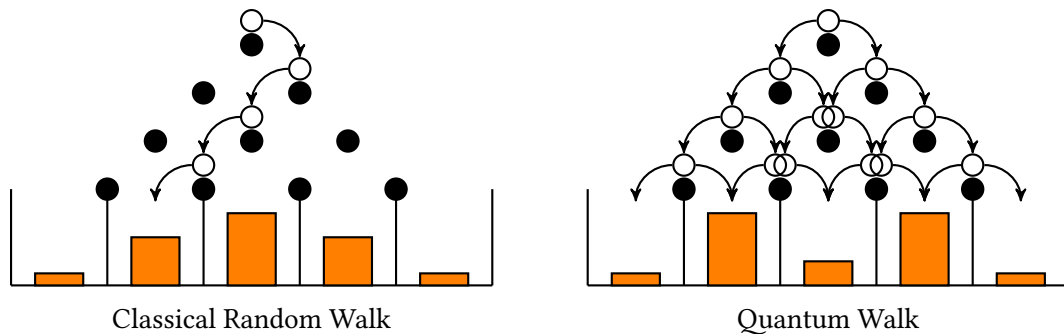
Figure 1.5.: Comparison of single trajectory of a classical random walk and a quantum walk using the example of a one-dimensional Galton board with resulting probability distributions.

The quantum-mechanical nature of the system will provoke interference effects between the correlated positions. The appearance of interference fringes makes the probability distribution of the final positions drastically different from the one of classical random walks. The consequences of the interference strongly depends on the choice of the coin operator and also on the initial internal state but generally one will find destructive interference near the origin of the distribution and constructive one towards the edges. Another major difference between the classical random walk and the quantum walk is how their standard deviation scales with the number of steps taken in the walk. Classically it scales with $\sqrt{N}$ and in the quantum case with N.

Quantum walks are also interesting to field of quantum-to-classical transitions. If one introduces decoherence in a quantum walk, the destruction of the coherence, the walk becomes classical again. Hence such a quantum walk might be used as a decoherence sensor. Small amounts of decoherence may also be used to tune certain characteristics (spreading for example) of the walk, that lead better than pure quantum dynamics in certain algorithms [27].

1.2.2. Quantum Walks in Momentum Space

The experiment consists of ultra-cold Rubidium 87 atoms in a Bose-Einstein condensate. The two degrees of freedom of this quantum walks scheme are the external centre-of-mass momentum of the atoms and the internal hyperfine state. The Rubidium atom is a three-levels system of one excited state $5\,^2P_{\frac{3}{2}}, F = 3$ and two ground states $5\,^2S_{\frac{1}{2}}, F = 1$ and $5\,^2S_{\frac{1}{2}}, F = 2$. The two ground states will be our internal degree of freedom. For the remainder of this thesis we shall rename the hyperfine levels for reasons of brevity:

$$|5\,^2S_{\frac{1}{2}}, F = 1\rangle \rightarrow |2\rangle \tag{1.32}$$

$$|5\,^2S_{\frac{1}{2}}, F = 2\rangle \rightarrow |1\rangle \tag{1.33}$$

$$|5\,^2P_{\frac{3}{2}}, F = 3\rangle \rightarrow |e\rangle \tag{1.34}$$

The internal degree states are addressed by the two-parameter unitary rotation matrix which in the experiment is done by microwaves

$$M(\alpha, \chi) = \begin{pmatrix} \cos\frac{\alpha}{2} & e^{-i\chi}\sin\frac{\alpha}{2} \\ -e^{i\chi}\sin\frac{\alpha}{2} & \cos\frac{\alpha}{2} \end{pmatrix}. \tag{1.35}$$

Initially we prepare a quantum ratchet state in one of the two possible internal levels, for example $|1\rangle$ and in a ratchet fashion in reciprocal space. In this thesis we will only consider initial momentum states of the form of (1.26). Additionally the relative phase is fixed to $\phi =$

$-\frac{\pi}{2}$ so that for kick strengths $k \approx 2$ the average momentum change per kick is near to unity.

$$|\psi_2(-\frac{\pi}{2})\rangle = \frac{1}{\sqrt{2}}(|n=0\rangle - i|n=1\rangle) \tag{1.36}$$

Note that, for such an asymmetric state, the mean momentum is not zero and therefore the resulting quantum walk will not be centred around zero but, here in this case, at one half momentum units. This initial state is then brought into a superposition in its internal degree of freedom with the Hadamard gate:

$$M(\alpha = \frac{\pi}{2}, \chi = 0)|2\rangle \otimes |\psi_2(-\frac{\pi}{2})\rangle = \frac{1}{\sqrt{2}}(|1\rangle + |2\rangle) \otimes |\psi_2(-\frac{\pi}{2})\rangle \tag{1.37}$$

Each step of the quantum walks starts with a pulse of the optical lattice kicking the atoms to induce the momentum change. In contrast to previous normal atom optics kicked rotor set-ups the standing wave laser is tuned between the two ground state levels so that one is negatively and one positively detuned. The sign of the detuning directly translates into the sign of the kick strength [24] via

$$k = \frac{\Omega^2 \tau_p}{8\Delta} \tag{1.38}$$

where Ω is the Rabi frequency, τ_p the pulse length of the kick and Δ the detuning. The standing-wave laser in the experiment is aligned in a $53°$ angle to the vertical, this changes the grating on the horizontal to

$$2k_L \rightarrow 2k_L \cdot 2\sin(53°). \tag{1.39}$$

And since the direction of the average momentum change depends on the sign of the kick strength we have achieved a conditional displacement. The following one-step operator $\hat{U}_{kick}$ that kicks carries this out depending on the total angular momentum.

$$U_{\text{kick}} = \begin{pmatrix} e^{-ik\cos\hat{\theta}} & 0 \\ 0 & e^{ik\cos\hat{\theta}} \end{pmatrix} \tag{1.40}$$

From this symmetric translation operation one can easily get to an asymmetric one by tuning the standing-wave laser closer to one level than the other:

$$U_{\text{kick}} = \begin{pmatrix} e^{-ik_1\cos\hat{\theta}} & 0 \\ 0 & e^{ik_2\cos\hat{\theta}} \end{pmatrix} \tag{1.41}$$

After each of these kicks mix the spin up and spin down states by applying the 50:50 beam-splitter coin toss

$$M(\alpha = \frac{\pi}{2}, \chi = -\frac{\pi}{2}) = \frac{1}{\sqrt{2}}\begin{pmatrix} 1 & i \\ i & 1 \end{pmatrix}. \tag{1.42}$$

Whether the walk will be symmetric or asymmetric only depends on the preparation and propagation of the internal degree of freedom which are determined by the choice of the initial state and the coin toss. In our case the initial state is symmetric in spin space. The coin behaves also in a symmetrical manner, the part of the created superposition in spin space that in the next kick will be send towards the edges of the distribution is multiplied with 1, therefore leading to constructive interference, while the part that will be kicked towards the centre is multiplied with i, which will after some iterations lead to cancellations, destructive interference. For that reason our walk will be symmetric.
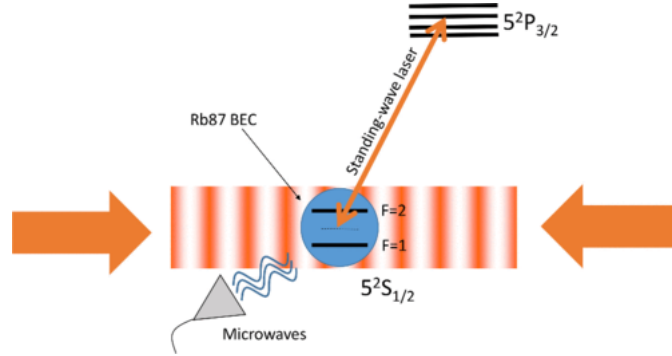
Figure 1.6.: Schematic of the proposed experiment for the realization of a quantum walk in momentum space. The optical lattice is pulsed periodically to implement the momentum shifts at quantum resonance. The internal states F = 1 and F = 2 of the atoms in the rubidium-87 condensate are controlled by microwaves. Taken from [7].

Experimentally one has access to the internal-state resolved momentum distribution. The total momentum distribution is computed from the sum of the momentum distribution of the two ground states.

$$P(n;T) = P_1(n;T) + P_2(n;T) \tag{1.43}$$

2. Numerical Implementation

2.1. Quantum Map

The averaged momentum distribution is computed via numerical simulations more precisely a Monte Carlo simulation that we will shortly describe in the following section [28].

We have a finite basis of position and momentum classes of length N where N is chosen to be a power of two so that we may use the fast Fourier Transform "four1" from Numerical Recipes [29] without further complications. This creates the following grid of position classes

$$\theta_i = \frac{2\pi}{N} i \tag{2.1}$$

and momentum classes

$$n = -\frac{N}{2}, -\frac{N}{2} + 1, ..., \frac{N}{2} - 1. \tag{2.2}$$

Instead of simulating a single two component wave function, each of our ground levels has its own wave function. Because of the complex nature of wave function we allocate an array of twice the base size for them and store the real part in the even and the complex part in the odd spaces.

An initial state in a quantum ratchet fashion as described in (1.36) would be given by:

$$\begin{aligned}
\psi_1(N) &= \frac{1}{\sqrt{2}} \\
\psi_1(N+3) &= -\frac{1}{\sqrt{2}} \\
\psi_2(N) &= \frac{1}{\sqrt{2}} \\
\psi_2(N+3) &= -\frac{1}{\sqrt{2}}
\end{aligned} \tag{2.3}$$

The kick-to-kick time evolution operator is composed of two parts: a kick part

$$K = e^{-ik\cos\theta} \tag{2.4}$$

and a free evolution part

$$F = e^{-\frac{i}{2}\tau n^2}. \tag{2.5}$$

This peculiar form of makes it difficult to compute both parts in one space. Both parts are easily computed in position and momentum space respectively. Therefore during a single step of a kick sequence, after having applied the free evolution, the wave function is Fourier transformed into position space and the kick is performed. Afterwards we transform back to momentum space. This is iteratively done T times, the amount of kicks performed on the system. Note that one wave function is kicked with k and the other with $-k$.

For our purposes we have to reorder by switching the order of the halves of the resulting array (FFT-shift) after the transformation from (angular) momentum space to (angular) position space and when transforming back because our momenta n are centred around 0 and our angles θ around π.

We get the momentum distribution P of one realisation by computing:

$$P(n;T) = \frac{1}{2} \left[|\psi_1(n;T)|^2 + |\psi_2(n;T)|^2 \right] \tag{2.6}$$

Note that we have to divide by two here because we work with two wave functions that are both normalized and not two components of one wave function.

If we additionally to these dynamics, consider the influence of stochastic decoherence effects (see the next three sections), we have to compute the quantum trajectory and the resulting momentum distribution for each atom. In a final step we form a classical average $\bar{P}$ over a given number of realizations R in a Monte Carlo method fashion.

$$\bar{P} = \frac{1}{R} \sum_{r=1}^{R} P_r \tag{2.7}$$

2.2. Monte Carlo Wave Function Technique

The Monte Carlo wave function method, also known as Quantum jump method, is a technique developed by Mølmer, Castin and Dalibard in the 90s to simulate Master equations [30]. The main idea behind it is to reduce the computation resources by computing solely the wave function instead of the density matrix, thus the needed resources only scale with $\mathcal{O}(N)$, if N is the dimensionality of the system, rather than with $\mathcal{O}(N^2)$.

As above we work in dimensionless units (in particular $\hbar = 1$). Let us assume that we have a system that is described by the Master equation

$$\rho = i \left[\rho, H \right] - \frac{1}{2} \sum_i \left(L_i^\dagger L_i \rho + \rho L_i^\dagger L_i \right) + \sum_i L_i^\dagger \rho L_i \tag{2.8}$$

start at an instant t in time with a wave function $|\psi(t)\rangle$.

$$H_{\text{jump}} = H - \frac{i}{2} \sum_m L_m^\dagger L_m \tag{2.9}$$

The quantum state evolves in time according to:

$$|\psi(t + \delta t)\rangle = e^{-iH_{\text{jump}}\delta t}|\psi(t)\rangle \tag{2.10}$$

because H might be a big full matrix the computation of its matrix exponential can become difficult. This is why we will Taylor expand it to first order.

$$|\psi(t + \delta t)\rangle = \left(1 - iH_{\text{jump}}\delta t\right)|\psi(t)\rangle \tag{2.11}$$

This is only valid if $H_{\text{jump}}t$ is small, which is not the case for the time evolution during the kick as the exponent of $e^{-ik\cos\hat\theta}$ can be quite big. This problem can be solved by using the following fundamental property of the matrix exponential:

$$e^{-iH_{\text{jump}}t} = \left[e^{-iH_{\text{jump}}t/s}\right]^s \tag{2.12}$$

and splitting the duration of the kick pulse into a large number of steps s for which each then the exponent is small enough to approximate the matrix exponential linearly.

The norm of the wave function decreases while evolving with the Hamiltonian because of its non-Hermiticity, the norm is equal to

$$\begin{aligned}
\langle\psi(t + \delta t)|\psi(t + \delta t)\rangle &= \langle\psi(t)|\left(1 + iH_{\text{jump}}^\dagger\delta t\right)\left(1 - iH_{\text{jump}}\delta t\right)|\psi(t)\rangle \\
&= \langle\psi(t)|1 - i\left(H_{\text{jump}} - H_{\text{jump}}^\dagger\right)\delta t + H_{\text{jump}}^\dagger H_{\text{jump}}\delta t^2|\psi(t)\rangle \\
&= 1 - \delta p + \mathcal{O}(\delta t^2)
\end{aligned} \tag{2.13}$$

where

$$\delta p = i\delta t\langle\psi(t)|\left(H_{\text{jump}} - H_{\text{jump}}^\dagger\right)|\psi(t)\rangle = \sum_m \delta p_m \tag{2.14}$$

can be written as a sum of

$$\delta p_m = \delta_t\langle\psi(t)|L_m^\dagger L_m|\psi(t)\rangle. \tag{2.15}$$

Now we have to decide whether a quantum jump happened. For this a random number η is drawn from an uniform distribution between 0 and 1. If this number is bigger than δp no quantum jump occurs we simply take the wave function after evolution with the time evolution operator and normalize it:

$$|\psi(t + \delta t)\rangle = \frac{1}{\sqrt{1 - \delta p}}\left(1 - iH_{\text{jump}}t\right)|\psi(t)\rangle \tag{2.16}$$

If on the other hand this number is smaller than δp then a quantum jump through one of the decoherence channels happens:

$$|\psi(t + \delta t)\rangle = \sqrt{\frac{\delta t}{\delta p_m}} L_m |\psi(t)\rangle \tag{2.17}$$

with a probability $\frac{\delta p_m}{\delta p}$.

2.3. Taking into account the Recoil

As mentioned earlier absorbing or emitting a photon induces a translation of the atomic momentum. The velocity change corresponds to the energy difference from the excited state to one of the ground states depending on the decay channel. Since we are only interested in a one-dimensional walk we have to project onto the walk axis. More on the atomic recoil can be found in section 5.2 and subsection 5.3.4.

Normally we have a difference in the ranges of possible momentum changes as we have the different energy differences. Since the detuning is very small in comparison to the transition frequency and we also have the projection as a diminishing factor we ignore this difference in the following and assume that both decay channels happen on with a recoil of $\hbar k_L$, this corresponds to a half of our momentum units.

The two-fold nature of the momentum in the atom optics kicked rotor forces us to deal the integer and fractional part of the momentum separately. Let ξ be the projection on the walk axis of the spontaneous emission recoil, then the wave function in momentum space is shifted by the integer part of the sum of ξ and the quasimomentum before the spontaneous emission β. It can change at most by one momentum class

$$n' = \begin{cases} 1 & \beta + \xi \geq 1 \\ 0 & 1 > \beta + \xi \geq 0 \\ -1 & \beta + \xi < 0 \end{cases} \tag{2.18}$$

The old quasimomentum is just replaced by the remaining fractional part

$$\beta' = \begin{cases} \beta + \xi - 1 & \beta + \xi \geq 1 \\ \beta + \xi & 1 > \beta + \xi \geq 0 \\ \beta + \xi + 1 & \beta + \xi < 0 \end{cases} \tag{2.19}$$

2.4. Taking into account the Quasimomentum

The atoms of the Bose-Einstein condensate after their initial preparation due to experimental limitations do not all have the same momentum but rather follow a normal distribution. The width of this Gaussian is fairly small so that effectively all atoms still belong to the $n = 0$ momentum class. The distribution is just a distribution of the quasimomenta β with a full width at half maximum Δ_β.

Since we already do quantum trajectories because of the spontaneous emission we can simply take into account the finite width in quasimomentum by drawing for each atom, so at the start of each realization, a random β.

See section 3.3 where this is applied to simulate the experimental data.

3. Theoretical treatment of the system

3.1. Overview

The experiment described in the subsection 1.2.2 can, in few-level approximation, be reduced to an atomic three-level system in Λ-constellation, with an upper level $|e\rangle$ and two lower levels $|1\rangle$ and $|2\rangle$. See figure (3.1) for a schematic representation of the reviewed system.
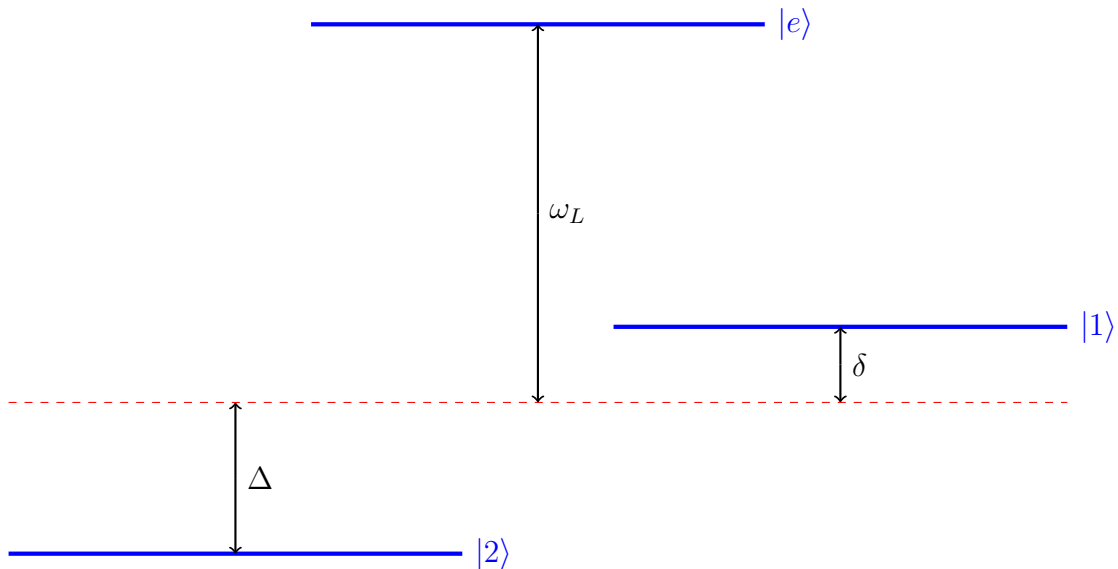
Figure 3.1.: Schematic representation of the system at hand as an atom in Λ-configuration.

The free atom Hamiltonian is composed of two parts, one describing the internal dynamics

$$H_0 = \hbar\omega_1|1\rangle\langle1| + \hbar\omega_2|2\rangle\langle2| + \hbar\omega_e|e\rangle\langle e| \tag{3.1}$$

plus one centre-of-mass motion part

$$H_{c.m} = \frac{\hat{p}^2}{2M}, \tag{3.2}$$

where the ω_i are the atomic frequencies of the different levels and $\hat{p}$ is the momentum of the atom of mass M.

The standing wave laser which kicks atoms can be written as the sum of two waves travelling

against each other [17]

$$\vec{E}(\hat{x}, t) = \hat{z} E_0 \left[\cos(k_L \hat{x} - \omega_L t) + \cos(k_L \hat{x} + \omega_L t) \right] \tag{3.3}$$

$$= \hat{z} E_0 \cos(k_L \hat{x}) \left(e^{i\omega_L t} + e^{-i\omega_L t} \right). \tag{3.4}$$

Here E_0 designates the amplitude of both waves, $\hat{z}$ is the polarization unit vector in z-direction. k_L and ω_L are the wave vector and the frequency of the laser. We will refrain from explicitly adding the δ-like periodicity of the field and future resulting interaction terms to relieve the notation.

The standing wave laser is tuned between the two ground levels such that the following relationships connecting the detuning and atomic frequencies holds:

$$\omega_e - \omega_1 = \omega_L - \delta \tag{3.5}$$

$$\omega_e - \omega_2 = \omega_L + \Delta \tag{3.6}$$

The wave length of the standing-wave laser is minimally detuned from the transitions between the excited and the ground states. This results, for a typical experiment with a Rubidium 87 Bose-Einstein condensate [17, 24], in a wave length in the optical regime

$$\lambda = 780 \text{nm}. \tag{3.7}$$

Hence the electrical field varies little over the space occupied by the atom and we can use the dipole approximation. In this approximation the atom-field Hamiltonian is given by:

$$H_1 = -\vec{d}\vec{E} \tag{3.8}$$

$$= \frac{\hbar \Omega_1}{2} \cos(k_L \hat{x}) \left(|1\rangle\langle e| e^{i\omega_L t} + |e\rangle\langle 1| e^{-i\omega_L t} \right)$$
$$+ \frac{\hbar \Omega_2}{2} \cos(k_L \hat{x}) \left(|2\rangle\langle e| e^{i\omega_L t} + |e\rangle\langle 2| e^{-i\omega_L t} \right), \tag{3.9}$$

where we identified Ω_1 and Ω_2 as the Rabi frequencies

$$\Omega_1 = -\frac{2\langle e|d_z|1\rangle E_0}{\hbar} \tag{3.10}$$

and

$$\Omega_2 = -\frac{2\langle e|d_z|2\rangle E_0}{\hbar} \tag{3.11}$$

which both are assumed to be real.

To get to (3.9) we first eliminated all symmetric terms for parity reasons as the dipole operators is uneven. In the next step we used the rotating wave approximation to eliminate

rapidly oscillating terms, which consists in removing terms which oscillate rapidly.

This is only possible if the laser is not too far detuned from resonance. Indeed this is the case, the detuning Δ and δ of the laser are also in the GHz-regime [7, 24] and therefore minuscule to the THz of the atomic transition frequencies.

$$\Delta = \delta \approx 2\pi \cdot 6.8\text{GHz} \ll \omega_0 \approx 2\pi \cdot 384.23\text{THz} \tag{3.12}$$

For the derivation of the effective Hamiltonian we need the interaction Hamiltonian in the interaction picture.

$$H_{\text{int}} = e^{\frac{i}{\hbar}H_0 t}\hat{H}_1 e^{-\frac{i}{\hbar}H_0 t} \tag{3.13}$$

$$\begin{aligned} &= \frac{\hbar\Omega_1}{2}\cos(k_L\hat{x})\left(|1\rangle\langle e|e^{i(\omega_L+\omega_1-\omega_e)t} + |e\rangle\langle 1|e^{-i(\omega_L+\omega_1-\omega_e)t}\right) \\ &+ \frac{\hbar\Omega_2}{2}\cos(k_L\hat{x})\left(|2\rangle\langle e|e^{i(\omega_L+\omega_2-\omega_e)t} + |e\rangle\langle 2|e^{-i(\omega_L+\omega_2-\omega_e)t}\right) \end{aligned} \tag{3.14}$$

$$\begin{aligned} &= \frac{\hbar\Omega_1}{2}\cos(k_L\hat{x})\left(|1\rangle\langle e|e^{i\delta t} + |e\rangle\langle 1|e^{-i\delta t}\right) \\ &+ \frac{\hbar\Omega_2}{2}\cos(k_L\hat{x})\left(|2\rangle\langle e|e^{-i\Delta t} + |e\rangle\langle 2|e^{i\Delta t}\right) \end{aligned} \tag{3.15}$$

where we made use of equation (3.5) in the last step. Note that the free evolution is not included in the unperturbed Hamiltonian because the kicks and the free evolution are assumed to happen at different times, see subsection 1.1.2.

3.2. Derivation of the Effective Hamiltonian

The interaction Hamiltonian (3.15) we got in the previous section is governed by terms that rapidly change in time. The theoretical framework of effective Hamiltonian theory deals with the question whether such Hamiltonians can be reduced to an simpler effective Hamiltonian without fast time oscillations. James et al. developed a simple compact formula in [34] which we will use in the following. See appendix C for a small summary of the derivation of this formula. Before its application we need to check whether the prerequisites for effective Hamiltonian theory are met:

First of all the atom-field interaction strength between field and atom has to be weak since this allows us to cut the expansion of the time evolution operator after the first order. In this case our small parameter are the Rabi frequencies which are for the usual kick strengths of around two in the order of magnitude of one GHz which is sufficiently lower than the atomic transition frequencies.

Secondly, the rapidly oscillating terms have to be able to be ignored. This is possible in rotating

wave approximation if the frequency of the laser field is near to the atomic transition frequencies which we already accounted for earlier, see previous section around equation (3.12).

And finally the atom-field interaction has to take place over a long period of time. This is a somewhat problematic since the length of the individual kick pulses is fairly short with approximately 100ns-1μs [24]. But the length of the whole kick sequence exceeds the lifetime of the transitions which are about 26ns [35] by a factor of at least 50, which should suffice.

Our interaction Hamiltonian (3.15) has an harmonic time dependence and can be written in the following form:

$$H_{\text{int}} = \sum_{n=1}^{2} \left(h_n e^{-i\nu_n t} + h_n^\dagger e^{i\nu_n t} \right),$$ (3.16)

with

$$h_1 = \frac{\hbar\Omega_1}{2} \cos(k_L \hat{x}) |e\rangle\langle 1|$$
$$h_2 = \frac{\hbar\Omega_2}{2} \cos(k_L \hat{x}) |2\rangle\langle e|$$
$$\nu_1 = \delta$$
$$\nu_2 = \Delta.$$ (3.17)

For Hamiltonians of this form, according to [34], the effective Hamiltonian can simply be computed by

$$H_{\text{eff}} = \sum_{m,n=1}^{2} \frac{1}{\hbar\bar{\nu}_{mn}} \left[h_m^\dagger, h_n \right] e^{(i(\nu_m - \nu_n)t)}$$
$$= \frac{\hbar\Omega_1^2}{4\delta} \cos^2(k_L \hat{x}) \left(|1\rangle\langle 1| - |e\rangle\langle e| \right) + \frac{\hbar\Omega_2^2}{4\Delta} \cos^2(k_L \hat{x}) \left(|e\rangle\langle e| - |2\rangle\langle 2| \right).$$ (3.18)

Let us now compare our effective Hamiltonian with the results derived in [33, 34] for similar systems. Note that the sign difference in the second part of our effective Hamiltonian comes from the fact that one of our detuning is negative. An important difference of our result from [33, 34] is the fact that transitions between the two lower levels $|1\rangle$ and $|2\rangle$ vanishes in our case. Since those transitions are dipole-forbidden this is in accord with what we expected. But it is possible to have an effective coupling via the excited state, leading to coherent oscillations between their populations like in [34]. Again our negative detuning is the reason because of which we do not get these terms. If we impose one detuning to be negative in [33] the prefactor to those transitions would go as $\Omega_1\Omega_2 \frac{\delta - \Delta}{\delta\Delta}$ and clearly disappear for two detunings close in amplitude. Analogously in [34] one negative detuning changes their time dependence from $e^{\pm i(\Delta - \delta)t}$ to $e^{\pm i(\Delta + \delta)t}$, so that the terms cancel by the time averaging procedure. So our result is in consensus with the other works of the field.

Because the excited state $|e\rangle$ is on average not populated as the lifetime of $|e\rangle$ is very short with 26 ns we can throw those out of the last equation to arrive at

$$H_{\text{eff}} = \frac{\hbar\Omega_1^2}{4\delta}\cos^2(k_L\hat{x})|1\rangle\langle1| - \frac{\hbar\Omega_2^2}{4\Delta}\cos^2(k_L\hat{x})|2\rangle\langle2|. \tag{3.19}$$

3.3. Relative Phases

The Hamiltonian that we have gotten in equation (3.19) has not yet the desired form shown in (1.40). In the 'classical' atom optics kicked rotor formalism one uses the fact that the squared cosine may be rewritten using the trigonometrical relation

$$\cos^2(\alpha) = \frac{1}{2}\left(\cos(2\alpha) + 1\right). \tag{3.20}$$

If we do this we get

$$H_{\text{eff}} = \frac{\Omega_1^2 \frac{1}{2}\left[\cos(2k_L\hat{x}) + 1\right]}{4\delta}|1\rangle\langle1| - \frac{\Omega_2^2 \frac{1}{2}\left[\cos(2k_L\hat{x}) + 1\right]}{4\Delta}|2\rangle\langle2| \tag{3.21}$$

$$= \left(\frac{\Omega_1^2\cos(2k_L\hat{x})}{8\delta} + \frac{\Omega_1^2}{8\delta}\right)|1\rangle\langle1| - \left(\frac{\Omega_2^2\cos(2k_L\hat{x})}{8\Delta} + \frac{\Omega_2^2}{8\Delta}\right)|2\rangle\langle2|. \tag{3.22}$$

The constant part of (3.20) leads to offset terms. In the normal kicked rotor such terms also appear. But here the typical kicked rotor is a two-level system of an excited and a ground state that after adiabatic elimination of the first becomes effectively a one-level system in which these terms can be disposed of by shifting the energy by a constant offset without changing the dynamics.

In our model we have a three-level system that after adiabatic elimination becomes a two-level one. The additional terms are different in sign because of their dependence on the detuning. Therefore we can no longer simply offset them and their existence will lead to a relative phases between the two internal levels in the time evolution:

$$U = e^{-iH_{\text{eff}}\tau_p} = \begin{pmatrix} e^{-i\left(\frac{\Omega_1^2\cos(2k_L\hat{x})}{8\delta} + \frac{\Omega_1^2}{8\delta}\right)} & 0 \\ 0 & e^{i\left(\frac{\Omega_2^2\cos(2k_L\hat{x})}{8\Delta} + \frac{\Omega_2^2}{8\Delta}\right)} \end{pmatrix} \tag{3.23}$$

This is not compatible with the ideal walk because of the drifting phase between the two internal-coin states! To make the difference between this kick operator to the one from the initial proposition clear we rewrite equation (3.23) in natural units and by identifying the kick strength from equation (1.38). Also the additional phases in both levels are consolidated to the

second level by a global multiplication with the additional phase in the first level:

$$
U = \begin{pmatrix} e^{-ik_1 \cos \hat{\theta}} & 0 \\ 0 & e^{ik_2 \cos \hat{\theta}} e^{i\Phi_{\text{kick}}} \end{pmatrix}
\tag{3.24}
$$

with a relative light shift phase that corresponds to the sum of kick strengths

$$
\Phi_{\text{kick}} = k_1 + k_2
\tag{3.25}
$$

$$
\underset{\Delta = \delta}{=} 2k.
\tag{3.26}
$$

Of course this is not the only relative phase between those levels. The energy difference between both creates also a dynamical phase shift

$$
\Phi_{\text{dyn}} = (\omega_1 - \omega_2)\tau
\tag{3.27}
$$

$$
\underset{\Delta = \delta}{=} 2\Delta\tau.
\tag{3.28}
$$

The total phase

$$
\Phi = \Phi_{\text{kick}} + \Phi_{\text{dyn}}
\tag{3.29}
$$

can be be compensated by a phase-shift gate acting on the internal states of the atom

$$
M(\pi, 0)M(\pi, \frac{\Phi}{2}) = \begin{pmatrix} 0 & -1 \\ 1 & 0 \end{pmatrix} \begin{pmatrix} 0 & e^{-i\frac{\Phi}{2}} \\ -e^{i\frac{\Phi}{2}} & 0 \end{pmatrix}
\tag{3.30}
$$

$$
= \begin{pmatrix} e^{i\frac{\Phi}{2}} & 0 \\ 0 & e^{-i\frac{\Phi}{2}} \end{pmatrix}.
\tag{3.31}
$$

We absorb this phase correction into the coin operator, leading to a new phase corrected coin

$$
C = M(\frac{\pi}{2}, -\frac{\pi}{2})M(\pi, 0)M(\pi, \frac{\Phi}{2})
\tag{3.32}
$$

$$
= \begin{pmatrix} 1 & i \\ i & 1 \end{pmatrix} \begin{pmatrix} e^{i\frac{\Phi}{2}} & 0 \\ 0 & e^{-i\frac{\Phi}{2}} \end{pmatrix}
\tag{3.33}
$$

$$
= \begin{pmatrix} e^{i\frac{\Phi}{2}} & ie^{-i\frac{\Phi}{2}} \\ ie^{i\frac{\Phi}{2}} & e^{-i\frac{\Phi}{2}} \end{pmatrix}.
\tag{3.34}
$$

(a) Without phase compensation (b) With phase compensation
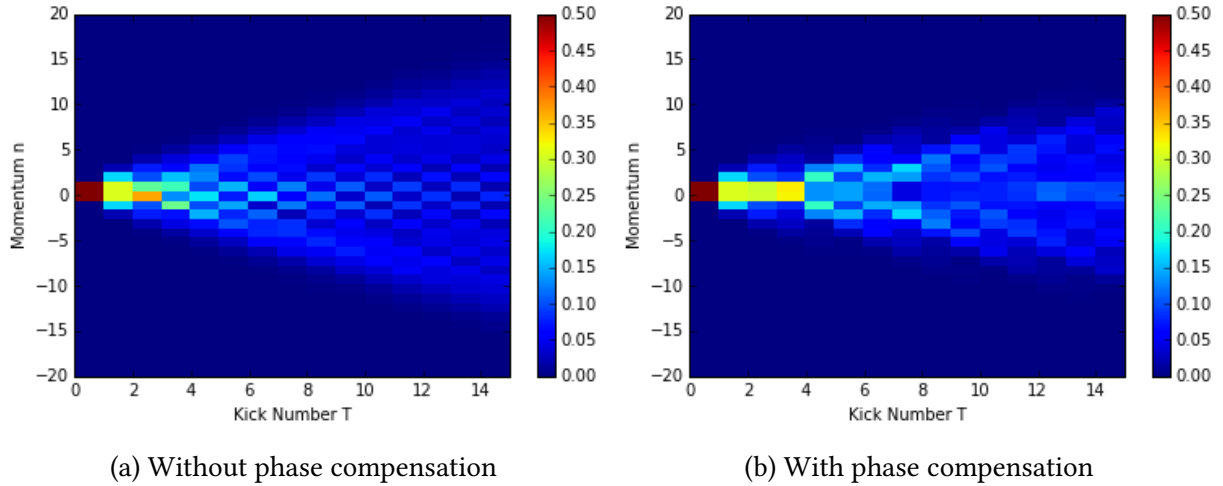
Figure 3.2.: Simulation of the effect of the phase for a quantum walk with $k = 1.4$ and $\Delta_\beta = 0.025$.

The numerics takes Δ_β, finite width of the quasimomenta, into account. The theoretical data shows that the additional phase leads to a broadening and an accumulation of weight in the centre of the momentum distribution. The dominant wings in (b) are no longer the maxima in (a), where they are in the centre.

(a) Without phase compensation (b) With phase compensation
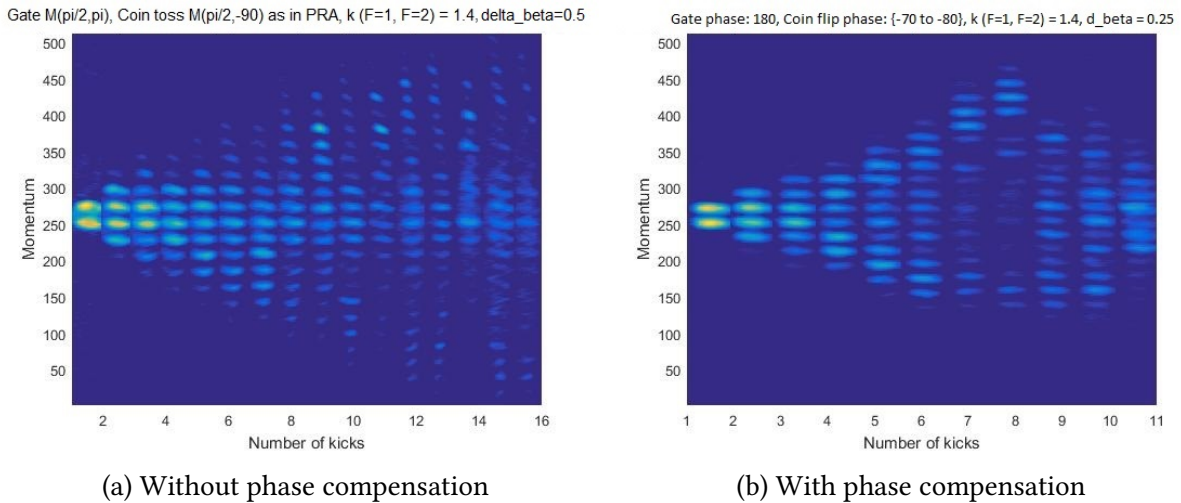
Figure 3.3.: Preliminary experimental data to the effect of the relative phase [38].

The preliminary experimental evidence is in qualitative agreement with the theoretical simulations. Small divergences can be explained by the fact that the exact value of the width in quasimomenta is unknown and we used an estimate $\Delta_\beta = 0.025$ for the numerics. The estimate is probably a little too low as the case without phase compensation is not as localized in the centre as in the experiment. Another hint at this is that the wings are more suppressed in (a) in the simulation.

But we also expect further decoherence effects to play a role here, such as spontaneous emission that will be treated in the upcoming chapter 5.

4. Investigation of the ideal case

In the previous chapter we have seen that the experiment, after correction of a relative phase, corresponds to the theoretical model described in subsection 1.2.2. Our first goal shall be to find an analytical solution for the momentum distribution of the quantum walk. Afterwards we will take a look how k and T influence the walk.

4.1. Analytical theory

We proceed by constructing the quantum walk with the time evolution operators that make it up in position space, and then in a final step Fourier transform to momentum space to get the momentum distribution.

A single step of the quantum walk consists in kicking the atoms and then mixing the internal states so the total time evolution operator is just the product of (1.42) and (1.40):

$$\hat{U}_{\text{tot}} = \hat{M}(\alpha = \frac{\pi}{2}, \chi = -\frac{\pi}{2})\hat{U}_{\text{kick}} \tag{4.1}$$

$$= \frac{1}{\sqrt{2}} \begin{pmatrix} e^{-ik\cos\hat{\theta}} & ie^{ik\cos\hat{\theta}} \\ ie^{-ik\cos\hat{\theta}} & e^{ik\cos\hat{\theta}} \end{pmatrix} \tag{4.2}$$

Let the walk be composed of T of such steps, then the whole walk can be simply described by the single-step evolution operator to the power T.

$$\hat{U}_{tot}^T = \left(\frac{1}{\sqrt{2}}\right)^T \begin{pmatrix} A_1^{(T-1)}(k) & A_2^{(T-1)}(k) \\ A_3^{(T-1)}(k) & A_4^{(T-1)}(k) \end{pmatrix} \tag{4.3}$$

where $A_1^{(N)}(k)$, $A_2^{(N)}(k)$, $A_3^{(N)}(k)$ $A_4^{(N)}(k)$ designate the matrix entries for U_{tot} for $N+1$ steps of the quantum walk and kick strength k. The index

$$N = T - 1 \tag{4.4}$$

of the $A_i^{(N)}(k)$ corresponds to the order of the recursive polynomials that they will depend on. The order of the polynomials is always one lower than the power of the time evolution operator, hence the shift.

From those four matrix entries we really only have to derive A_1 and A_2, as one can easily

see by taking a glance at the step-by-step change rule (how A_2 is constructed from A_1 and A_2) that A_1 and A_2 are the same as A_4 and A_3 except for a sign change in k.

$$A_1^{(N)}(-k) = A_4^{(N)}(k) \tag{4.5}$$
$$A_2^{(N)}(-k) = A_3^{(N)}(k) \tag{4.6}$$

From explicitly writing down the first few matrix entries we found that they can be represented by recursive polynomials. A list of the first few matrix entries and a proof of the validity of this representation can be found in appendix B.

$$A_1^{(N)}(z) = e^{-ik\cos\hat\theta} p_1^{(N)}(z)$$
$$A_2^{(N)}(z) = ie^{ik\cos\hat\theta} p_2^{(N)}(z) \tag{4.7}$$

where the $p_1^{(N)}(z)$ and $p_2^{(N)}(z)$ are polynomials in the variable

$$z = e^{-ik\cos\hat\theta} + e^{ik\cos\hat\theta} \tag{4.8}$$

that are following the same recursion formula

$$p^{(N)}(z) = zp^{(N-1)}(z) - 2p^{(N-2)}(z) \tag{4.9}$$

but with different starting points:

$$p_1^{(0)}(z) = p_2^{(0)}(z) = 1 \tag{4.10}$$
$$p_1^{(1)}(z) = \tilde z \tag{4.11}$$
$$p_2^{(1)}(z) = z \tag{4.12}$$

where

$$\tilde z = e^{-ik\cos\hat\theta} - e^{ik\cos\hat\theta}. \tag{4.13}$$

The uniqueness of this definition is guaranteed by the recursion theorem. To solve this homogeneous linear recurrence relation with constant coefficients we substitute an ansatz $p^{(N)}(z) = x^N(z)$ in the recurrence relation (4.9) and solve the resulting quadratic equation.

$$x^N = zx^{N-1} - 2x^{N-2} \tag{4.14}$$
$$x^2 = zx - 2 \tag{4.15}$$
$$x_{1/2} = \frac{z \pm \sqrt{z^2 - 8}}{2} \tag{4.16}$$

Because of the linearity of the recurrence the general solution is

$$p_{1/2}^{(N)}(z) = c_1 x_1^N + c_2 x_2^N, \tag{4.17}$$

where c_1 and c_2 have to be chosen so that the starting conditions are fulfilled:

$$p_1^{(N)}(z) = \frac{1}{2}\left(1 + \frac{2\tilde{z} - z}{\sqrt{z^2 - 8}}\right)\left(\frac{z + \sqrt{z^2 - 8}}{2}\right)^N \tag{4.18}$$

$$+ \frac{1}{2}\left(1 - \frac{2\tilde{z} - z}{\sqrt{z^2 - 8}}\right)\left(\frac{z - \sqrt{z^2 - 8}}{2}\right)^N \tag{4.19}$$

$$p_2^{(N)}(z) = \frac{1}{2}\left(1 + \frac{z}{\sqrt{z^2 - 8}}\right)\left(\frac{z + \sqrt{z^2 - 8}}{2}\right)^N \tag{4.20}$$

$$+ \frac{1}{2}\left(1 - \frac{z}{\sqrt{z^2 - 8}}\right)\left(\frac{z - \sqrt{z^2 - 8}}{2}\right)^N \tag{4.21}$$

As all this is still in position space and in the end we are interested in being in momentum space we need to perform a Fourier transform back to it. We rewrite (4.18) and (4.20) in a form which is can be more easily transformed, for example as a sum of kick operators which translates into Bessel functions in reciprocal space:

$$p(z) \approx \sum_{j=0}^{N} e^{ijk\cos\hat{\theta}} \tag{4.22}$$

The calculations for this rewriting being long and tedious have been moved to appendix B. The results of this procedure are:

$$p_1^{(N)}(z) = \frac{1}{2^N}\left[\sum_{j=0}^{\frac{N}{2}}\sum_{m=0}^{j}\sum_{l=0}^{N-2m}\left(\binom{N}{2j} - \binom{N}{2j+1}\right)\binom{j}{m}\binom{N-2m}{l}e^{ik\cos\hat{\theta}(N-2m-2l)}(-8)^m\right]$$

$$- \frac{1}{2^N}2\left[\sum_{j=0}^{\frac{N}{2}}\sum_{m=0}^{j}\sum_{l=0}^{N-2m-1}\binom{N}{2j+1}\binom{j}{m}\binom{N-2m-1}{l}e^{ik\cos\hat{\theta}(N-2m-2l)}(-8)^m\right]$$

$$+ \frac{1}{2^N}2\left[\sum_{j=0}^{\frac{N}{2}}\sum_{m=0}^{j}\sum_{l=0}^{N-2m-1}\binom{N}{2j+1}\binom{j}{m}\binom{N-2m-1}{l}e^{ik\cos\hat{\theta}(N-2m-2l-2)}(-8)^m\right]$$

$$= \sum_{l=0}^{N} a_{l,A_1}e^{ik\cos\hat{\theta}(N-2l)}$$

$$p_2^{(N)}(z) = \frac{1}{2^N}\left[\sum_{j=0}^{\frac{N}{2}}\sum_{m=0}^{j}\sum_{l=0}^{N-2m}\binom{N+1}{2j+1}\binom{j}{m}\binom{N-2m}{l}e^{ik\cos\hat{\theta}(N-2m-2l)}(-8)^m\right]$$

$$= \sum_{l=0}^{N} a_{l,A_2}e^{ik\cos\hat{\theta}(N-2l)}$$

where

$$a_{l,1} = \frac{1}{2^N} \sum_{j=0}^{\frac{N}{2}} \left(\binom{N}{2j} - \binom{N}{2j+1} \right) \sum_{m=0}^{l} (-8)^m \binom{j}{m} \binom{N-2m}{l-m}$$

$$- \frac{1}{2^N} 2 \sum_{j=0}^{\frac{N}{2}} \binom{N}{2j+1} \sum_{m=0}^{l} (-8)^m \binom{j}{m} \binom{N-2m-1}{l-m}$$

$$+ \frac{1}{2^N} 2 \sum_{j=0}^{\frac{N}{2}} \binom{N}{2j+1} \sum_{m=0}^{l-1} (-8)^m \binom{j}{m} \binom{N-2m-1}{l-m-1}$$

$$a_{l,2} = \frac{1}{2^N} \sum_{j=0}^{\frac{N}{2}} \binom{N+1}{2j+1} \sum_{m=0}^{l} (-8)^m \binom{j}{m} \binom{N-2m}{l-m}$$

Consecutively for the matrix entries we have are:

$$A_1^{(N)}(k) = \sum_{l=0}^{N} a_{l,1} e^{ik\cos\hat{\theta}(N-2l-1)} \tag{4.23}$$

$$A_2^{(N)}(k) = i \sum_{l=0}^{N} a_{l,2} e^{ik\cos\hat{\theta}(N-2l+1)} \tag{4.24}$$

At this point we have everything to carry out the calculation of the momentum distribution.

4.1.1. Derivation of the Momentum distribution

The details of the calculation can be found again in appendix B. The final result is:

$$P(n;T) = \left[|\langle n,1|\psi_\beta(T)\rangle|^2 + |\langle n,2|\psi_\beta(T)\rangle|^2 \right]$$

$$= \frac{1}{2^{T+2}} \left[\left(\sum_{l=0}^{N} a_{l,1} \left[J_n((N-2l-1)k) - J_{n-1}((N-2l-1)k) \right] \right)^2 \right.$$

$$+ \left(\sum_{l=0}^{N} a_{l,2} \left[J_n((N-2l+1)k) - J_{n-1}((N-2l+1)k) \right] \right)^2$$

$$+ \left(\sum_{l=0}^{N} a_{l,1} \left[J_n(-(N-2l-1)k) - J_{n-1}(-(N-2l-1)k) \right] \right)^2$$

$$+ \left. \left(\sum_{l=0}^{N} a_{l,2} \left[J_n(-(N-2l+1)k) - J_{n-1}(-(N-2l+1)k) \right] \right)^2 \right]$$

Similar to how in a classical random walk for an even/uneven number of steps the walker will only be in a even/uneven position, the entry of the Bessel functions will only be an even/uneven multiple of k depending on the kick number.

4.1.2. Extension to more complex Ratchet States

The form of the ratchet is translated into the index of the Bessel functions, this formula can easily expanded to more complex ratchet states as long neighbouring momentum classes have relative phases of $\frac{\pi}{2}$ or $-\frac{\pi}{2}$.

$$\frac{1}{\sqrt{I}} \sum_{i=0}^{I} (-1)^i |n = n_i\rangle \rightarrow \frac{1}{2^{T+1}I} \Bigg[\left(\sum_{l=0}^{N} a_{l,1} \left[\sum_{i=0}^{I} (-1)^i J_{n-n_i}((N - 2l + 1)k) \right] \right)^2 \quad (4.25)$$

$$+ \left(\sum_{l=0}^{N} a_{l,2} \left[\sum_{i=0}^{I} (-1)^i J_{n-n_i}((N - 2l + 1)k) \right] \right)^2 \quad (4.26)$$

$$+ \left(\sum_{l=0}^{N} a_{l,1} \left[\sum_{i=0}^{I} (-1)^i J_{n-n_i}(-(N - 2l + 1)k) \right] \right)^2 \quad (4.27)$$

$$+ \left(\sum_{l=0}^{N} a_{l,2} \left[\sum_{i=0}^{I} (-1)^i J_{n-n_i}(-(N - 2l + 1)k) \right] \right)^2 \Bigg] \quad (4.28)$$

4.2. Simulation of the ideal case

First of all we want to check whether the analytical formula that we derived is in accordance with the numerical simulation via the quantum map that we have presented in section 3.1.
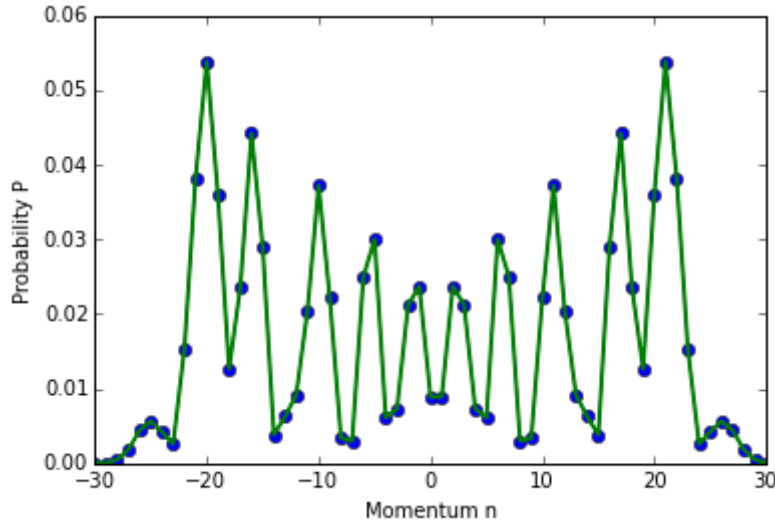
Figure 4.1.: Comparative plot of the numerically (blue dots) and analytically (green line) obtained momentum distribution for a quantum random walk with kick strength $k = 2$ and $T = 20$ steps.

As we can see there is compliance between our two ways of computing the momentum distributions.

We notice that in contrary to the simple quantum kicked rotor or even quantum ratchet the momentum distribution does no longer just depend on a single parameter kT, the product of

kick strength and number. The introduction of the coin to the system leads to the problem different sets of kick strengths and number of kicks with the same product result in disparate momentum distributions.
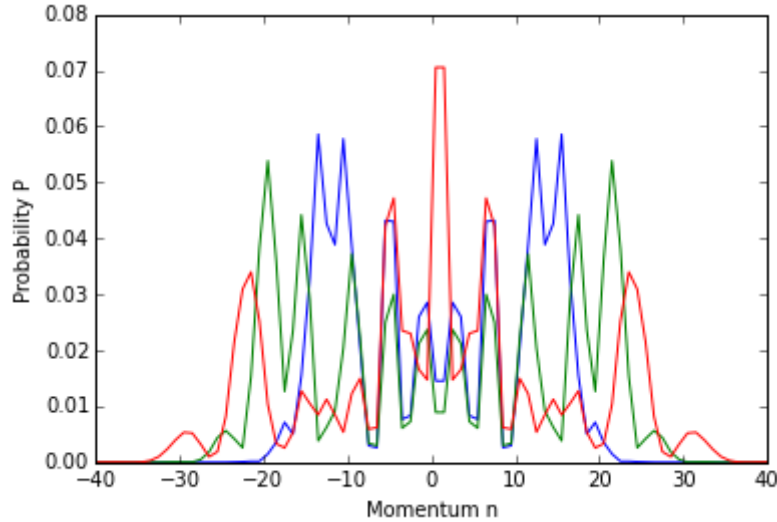
Figure 4.2.: Comparative plot of different quantum walks with same value for kT.

In the following we want to analyse how these two parameters (k, T) impact the momentum distribution.

4.2.1. Ballistic Expansion of the Walk

Let us now take a closer look at how the momentum distribution of the quantum walks behaves for different number of kicks. Similar to the simple quantum kicked rotor we observe two major peaks that linearly increase in time, ergo we have ballistic motion.

The width of the quantum walk (the distance of the maximum of the momentum distribution from its average) increases linearly with the kick number T. Also there is no limit to how many steps the walk can make without disappearing in contrast to the kick strength which is restricted to a small window as we will see later. The following measurements were created with $k = 2$ and increasing T.
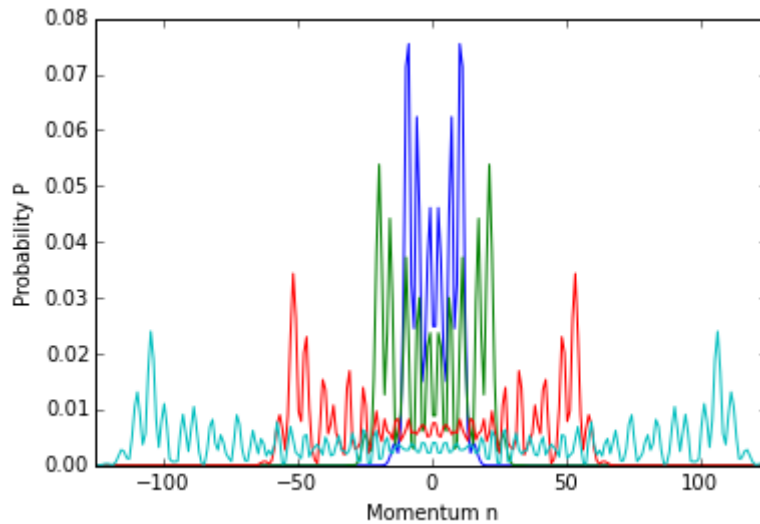
Figure 4.3.: Momentum distributions for walks for $k = 2$ with $T = 10$ (blue), $T = 20$ (green), $T = 50$ (red) and $T = 100$ (light blue).

We see that the number of kicks stretches the width of the walk, other than that it almost entirely conserves the structure of the walk. So the difference in the shape we observed earlier must come first and foremost from the kicks strength.
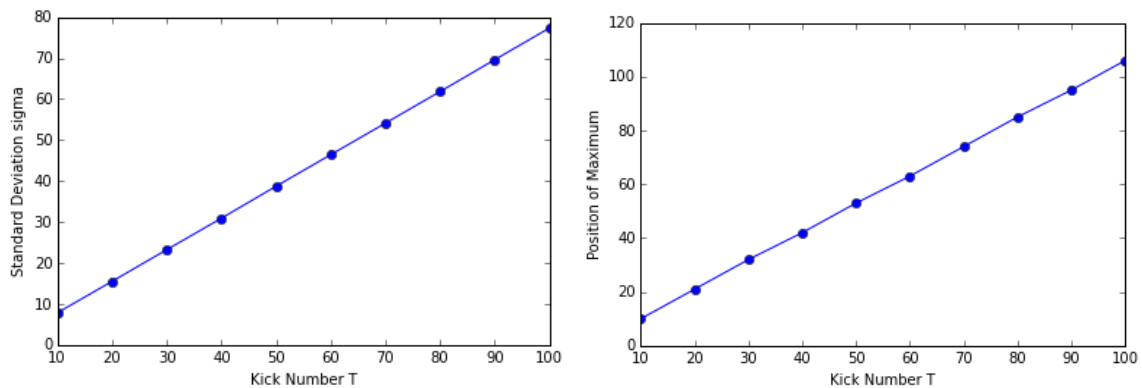
Standard deviation of the momentum distribution against the kick nuber T for a quantum walk with $k = 2$.

The right maximum of the momentum distribution against the kick nuber T for a quantum walk with $k = 2$.

The peaks show ballistic motion and the standard deviation growl linearly in time as expected for quantum walks, see preliminaries.

4.2.2. A Window for the Kick Strength

The following plots show the evolution in shape of the momentum distribution when varying the kick strength k. The number of steps is held constant at $T = 20$.
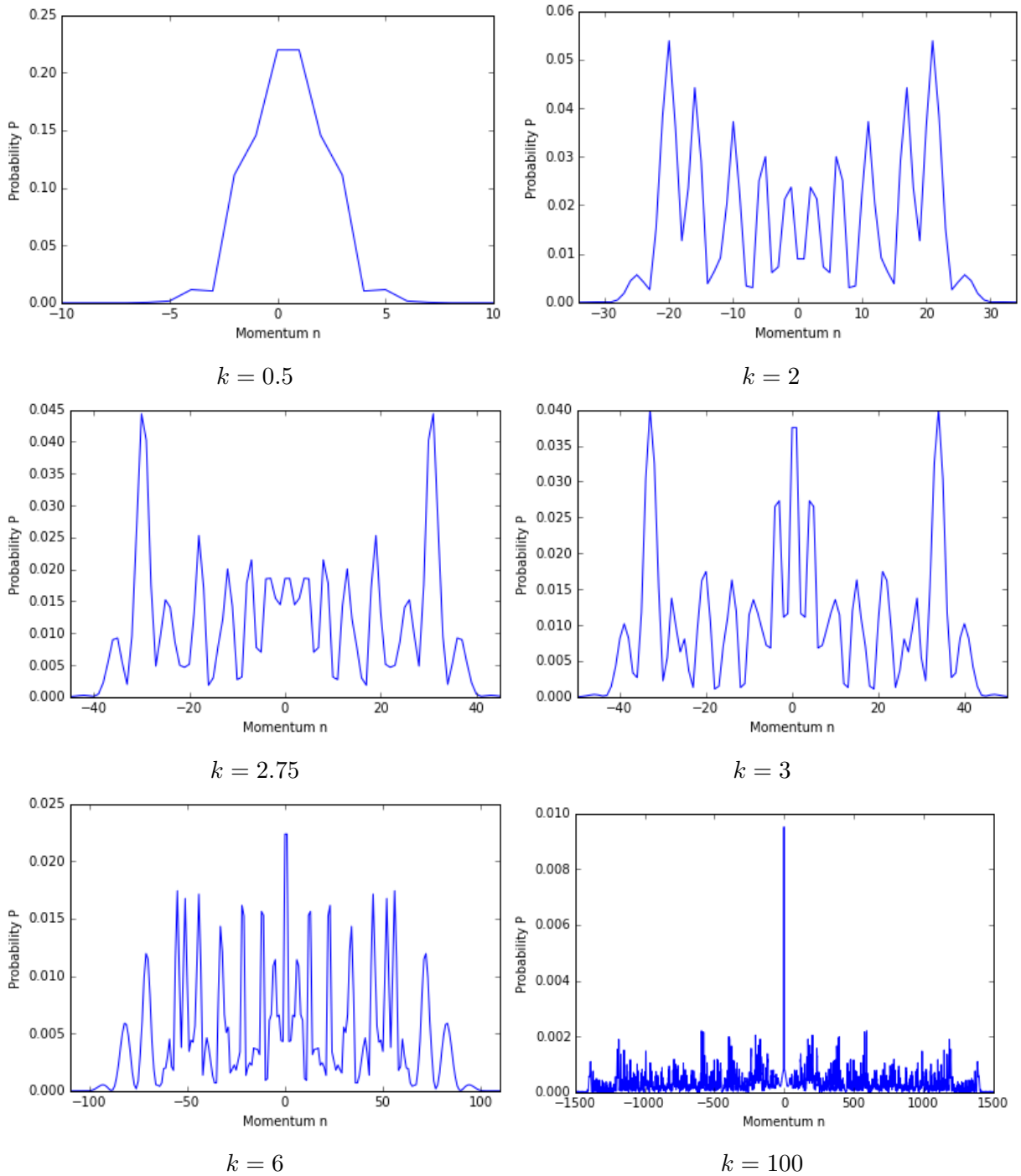
Figure 4.5.: Momentum distributions for walks for $T = 20$ for varying k.

The variation of the kick strength k shows that choosing a value far from the proposed value of $k = 2$ leads to momentum distribution without the 'typical shape' of a quantum walk. The typical walk being the one with the maxima being at the edges of the momentum distributions as shown in figure (4.5).

We observe that between $k = 2.75$ and $k = 3.0$ a peak emerges from the origin of the momentum distribution. This peak subsequently splits into two and then slowly diffuse towards

the edge of the distribution until near $k = 6$ the next peak emerges. The diffusion of the peak leads to a walk that loses its two clearly defined peaks at the edges and resembles more and more just noise.

We can observe that for too weak or powerful kicks the momentum distribution has its peaks in the centre. What happens is the following: If the kick strength is too weak, the overlap between neighbouring momentum classes is vanishing and the peak around the initial momentum classes simply does not diffuse. If k is too strong more distant momentum classes couple to one another by $J_{\Delta n}(k)$.

Our next goal will be to find a criterion, that allows us to say when a momentum distribution qualifies for being a 'good' quantum walk and when not. As an ad-hoc-solution we define a visibility in analogy to the interferometric visibility

$$v = \frac{P_{max} - P_{mid}}{P_{max} + P_{mid}}, \tag{4.29}$$

where P_{max} and P_{mid} denote the amplitude of the momentum distribution in the maximum and in the middle.

Concretely those two values are estimated by averaging the momentum distribution over a small segment of eight momentum classes around the momentum class with highest probability and the average momentum class respectively. The segments were chosen to be of equal length so that, when maximum and mean would coincide like for big kick strengths, P_{max} and P_{mid} are also equal and the visibility vanishes. We had to opt for a small number of momentum classes for the segments, as the local minima around the global maximum of the momentum distribution lie lower than the local minima in the centre of the distribution, thus leading to $P_{max} \ll P_{mid}$ which is not in the sense of our definition.
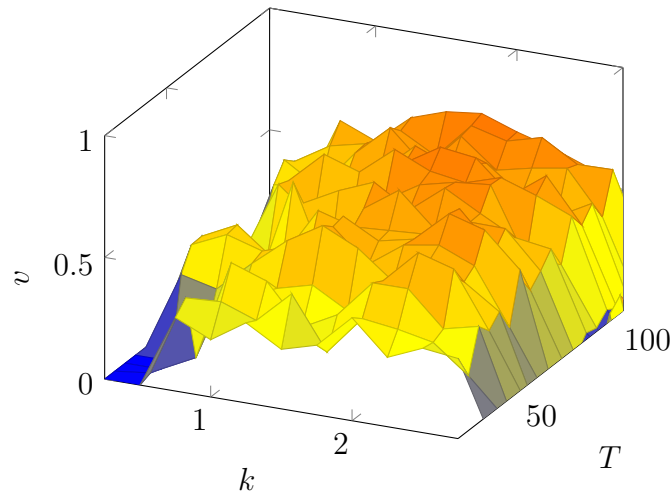
Figure 4.6.: Map of the visibility in dependence of the kick strength k and the number of kicks T.

From this graph we can extract that there is not really a limit to how many steps can make, although a certain minimum is advisable. Also we can see that the visibility increases with increasing number of kicks. The visibility falls of rapidly around $k = 0.75$ and $k = 2.75$. For kick strengths beyond $k = 3$ our definition fails since the maxima diffuse towards the edges of the walk but this is not that problematic since it suffices to find a first cutoff. For the ongoing investigation we shall restrict the kick strengths to a window of $k \in [0.75; 2.75]$.

5. Decoherence through Spontaneous Emission

The introduction of spontaneous emission to the system initiates the transition from a so far closed system to an open system. Open system may no longer be described by a unitary time evolution due to its dissipative nature. The usual course of action is to attack the problem by setting up an equation of motion for the density matrix called the master equation.

5.1. Setting up the Master equation

Until now we have ignored the environment and the coupling therewith. We consider our atomic system to be coupled to a vacuum environment. The coupling between the atoms and the quantized vacuum modes can be represented by the following Hamiltonian in the interaction picture

$$
\begin{aligned}
V_{\text{vac}}(t) = &\sum_{\vec{k}} g_{\vec{k}} \left(|e\rangle\langle 1| a_{\vec{k}} e^{-i(\nu_{\vec{k}} - (\omega_e - \omega_1))t} + |1\rangle\langle e| a_{\vec{k}}^{\dagger} e^{i(\nu_{\vec{k}} - (\omega_e - \omega_1))t} \right) \\
&+ \sum_{\vec{k}} g_{\vec{k}} \left(|e\rangle\langle 2| a_{\vec{k}} e^{-i(\nu_{\vec{k}} - (\omega_e - \omega_2))t} + |2\rangle\langle e| a_{\vec{k}}^{\dagger} e^{i(\nu_{\vec{k}} - (\omega_e - \omega_2))t} \right).
\end{aligned}
\tag{5.1}
$$

The full unitary and coherent evolution of the density matrix through time is given by the Liouville-von Neumann equation

$$
i\frac{\partial \rho(t)}{\partial t} = [V_{\text{vac}}(t), \rho(t)].
\tag{5.2}
$$

We integrate formally

$$
\rho(t) = \rho(t_0) - i \int_{t_0}^{t} [V_{\text{vac}}(t'), \rho(t')] \, dt'
\tag{5.3}
$$

and then we insert (5.3) into (5.2):

$$
\frac{\partial \rho(t)}{\partial t} = -i [V_{\text{vac}}(t), \rho(t_0)] - \int_{t_0}^{t} [V_{\text{vac}}(t) [V_{\text{vac}}(t'), \rho(t')]] \, dt'
\tag{5.4}
$$

On the way to the Master equation two important approximations are made: The first one is the Born approximation, a weak coupling condition. In its limit the total density matrix basically factorizes into an environment and an atomic part plus an additional assumed small

correction term ρ_c of order $\mathcal{O}(V^2)$

$$\rho = \rho_A \otimes \rho_{\text{vac}} + \rho_c. \tag{5.5}$$

Neglecting ρ_c we get

$$Tr_{\text{vac}}(\rho) = \rho_A. \tag{5.6}$$

By tracing out the environment, incoherent and irreversible dynamics arise.

$$\frac{\partial \rho_A(t)}{\partial t} = -iTr_{\text{vac}}\left[V_{\text{vac}}(t), \rho(t_0)\right] - \int_{t_0}^{t} Tr_{\text{vac}}\left[V_{\text{vac}}(t)\left[V_{\text{vac}}(t), \rho(t')\right]\right] dt' \tag{5.7}$$

The second is the Markov approximation which assumes that the environment when brought out of equilibrium goes back to it over very short time scales without being influenced from its coupling with the system so the environment stays constant and the history of the system does not influence the evolution. Quantitatively this requires that the decay rate, that gives the time scale of the coupling is way bigger than the time scale of the dynamics of the system given by the inverse optical frequency of the laser. This is easily satisfied in quantum-optical set ups [39]:

$$\gamma^{-1} \gg \omega_L^{-1} \tag{5.8}$$

This way we obtain the typical quantum-optical Master equation in Lindblad form [39]

$$\frac{d\rho}{dt} = -i\left[H, \rho\right] + \mathcal{D}[\rho] \tag{5.9}$$

with the dissipator superoperator:

$$\mathcal{D}[\rho] = -\frac{1}{2}\left(L_1^\dagger L_1 \rho_A(t) + \rho_A(t)L_1^\dagger L_1 - 2L_1\rho_A(t)L_1^\dagger\right) \tag{5.10}$$

$$-\frac{1}{2}\left(L_2^\dagger L_2 \rho_A(t) + \rho_A(t)L_2^\dagger L_2 - 2L_2\rho_A(t)L_2^\dagger\right) \tag{5.11}$$

with the Lindblad operators, also called Lindbladians:

$$\begin{aligned} L_1 &= \sqrt{\gamma_1}|1\rangle\langle e| \\ L_2 &= \sqrt{\gamma_2}|2\rangle\langle e| \end{aligned} \tag{5.12}$$

The Lindblad operators describe the decay from the excited towards one of the two ground states $|1\rangle$ and $|2\rangle$ with the spontaneous emission rate γ_1 or γ_2.

The spontaneous emission rates [40] can be computed from

$$\gamma_1 = \frac{k_1}{\tau_p \tau_{SE} \delta}$$
$$\gamma_2 = \frac{k_2}{\tau_p \tau_{SE} \Delta}$$

(5.13)

where τ_p is the pulse duration and τ_{SE} the life time of the transition [35].

5.2. Including the recoil motion of the atom

Up to now we have only have set up an Master equation that describes the evolution of the populations of the different internal states and neglected the atomic motional state. If we do a quantum walk it is of major importance. We add the missing centre-of-mass motion imitating the reasoning presented in [41].

From the Master equation in Lindblad form (5.10) we can derive via sandwiching equations for the populations and coherences:

$$\frac{\partial}{\partial t}\rho_{11} = \gamma_1 \rho_{ee}$$

(5.14)

$$\frac{\partial}{\partial t}\rho_{22} = \gamma_2 \rho_{ee}$$

(5.15)

$$\frac{\partial}{\partial t}\rho_{ee} = -\gamma_1 \rho_{ee} - \gamma_2 \rho_{ee}$$

(5.16)

$$\frac{\partial}{\partial t}\rho_{e2} = -\frac{\gamma_2}{2}\rho_{e2}$$

(5.17)

$$\frac{\partial}{\partial t}\rho_{e1} = -\frac{\gamma_1}{2}\rho_{e1}$$

(5.18)

$$\frac{\partial}{\partial t}\rho_{12} = 0$$

(5.19)

All these equations have no influence on the motional state of the atom. For the last four of them, the time decay of the excited state and the three coherences, this is correct. The reason for this is that the decay from the excited state is independent from its motional state and the decay does not have influence on the motional state of the excited state but rather on the ground state. Exactly this change of momentum in the ground state is missing in the decay from the excited state to the ground states, described in the first two equations.

An atom in the excited state $|e\rangle$ and momentum p will eventually decay into one of the ground states, while shifting its momentum by $\hbar k$ due to the recoil created when emitting a photon with momentum $\hbar k$. This momentum shift of the atom is described by the momentum-shift operator:

$$e^{-i\vec{\kappa}\cdot\vec{x}} = \int d^3p |\vec{p}\rangle\langle\vec{p} + \hbar\vec{\kappa}|$$

(5.20)

The emitted photons will because of the way our experiment is set up to tune the laser between both levels have wave vectors $\boldsymbol{\kappa}_1$ and $\boldsymbol{\kappa}_2$ of different length.

$$\kappa_1 = \frac{\omega_L - \delta}{c} \tag{5.21}$$

$$\kappa_2 = \frac{\omega_L + \Delta}{c} \tag{5.22}$$

We also have to account for the fact that the direction in which the photon is emitted via spontaneous emission is isotropically distributed.

$$\frac{\partial}{\partial t}\rho_{11} = \int d\gamma_1(\vec{n}_1)e^{-i\vec{\kappa}_1\vec{x}}\rho_{ee}e^{i\vec{\kappa}_1\vec{x}} \tag{5.23}$$

$$\frac{\partial}{\partial t}\rho_{22} = \int d\gamma_2(\vec{n}_2)e^{-i\vec{\kappa}_2\vec{x}}\rho_{ee}e^{i\vec{\kappa}_2\vec{x}} \tag{5.24}$$

where the $d\gamma_i(\vec{n}_i)$ are the differential rate of spontaneous emission given as a function of the unit vectors $\vec{n}_i$ of the emitted photon.

$$d\gamma_1(\vec{n}_1) = \gamma_1\Phi(\vec{n}_1)d^2\vec{n}_1 \tag{5.25}$$

$$d\gamma_2(\vec{n}_2) = \gamma_2\Phi(\vec{n}_2)d^2\vec{n}_2 \tag{5.26}$$

with the angular distribution density [41]

$$\Phi(\vec{n}) = \frac{3}{8\pi}\left[1 - (\vec{e}_p \cdot \vec{n})^2\right]. \tag{5.27}$$

where $\vec{e}_p$ is the unit vector of the atomic dipole transition moment.

The motion of atoms can have a non-negligible impact on the angular photon distribution emitted by spontaneous emission. In this formula (5.27) we have omitted two velocity depending contributions like Doppler shifts and the one that comes from adding the Röntgen term to the dipole approximation

$$H_R = -\frac{1}{2M}\left[\vec{p}\cdot\left(\vec{B} \times \vec{d}\right) + \left(\vec{B} \times \vec{d}\right)\cdot\vec{p}\right] \tag{5.28}$$

to account for the atomic motion [42].

The reason we could ignore these terms is that they scale with $\frac{v}{c}$ and the velocities of the atoms are very far from being relativistic. For comparison sake the velocity corresponding to a momentum unit is in the order of a couple millimetres per second.

The electric field of the standing wave laser points in the z-direction and forces the dipole element to align itself in the same direction. Therefore the atomic dipole transition moment

must show in the same direction. In the spherical coordinates the z- direction is just giving by a cosine.

$$\Phi(\phi, \theta) = \frac{3}{8\pi} \left[1 - \cos^2 \theta\right], \theta \in [0, \pi], \phi \in [0, 2\pi] \tag{5.29}$$

Since the walk takes place on the x-axis, only the x-component u of the recoil is going to matter. The distribution of $u = \cos(\phi)\sin(\theta)$ can be gotten from computing the distributions $f_v(v)$ and $f_w(w)$ of $v = \cos(\phi)$, $w = \sin(\theta)$ and the distribution of their product [43] via

$$\Phi(u) = \int_{-1}^{1} f_v(\frac{u}{w}) f_w(w) \frac{1}{|w|} dw, \tag{5.30}$$

which leads to

$$\Phi(u) = \frac{3}{8} \left[1 + u^2\right], u \in [-1, 1]. \tag{5.31}$$

Our Master equation taking also in consideration the momentum shifts changes to

$$\frac{\partial \rho_A(t)}{\partial t} = -\frac{1}{2} \left(L_1^\dagger L_1 \rho_A(t) + \rho_A(t) L_1^\dagger L_1 - 2 \int_{-1}^{1} du \Phi(u) L_1 e^{-iu\kappa_1 \hat{x}} \rho_A(t) e^{iu\kappa_1 \hat{x}} L_1^\dagger \right) \tag{5.32}$$

$$- \frac{1}{2} \left(L_2^\dagger L_2 \rho_A(t) + \rho_A(t) L_2^\dagger L_2 - 2 \int_{-1}^{1} du \Phi(u) L_2 e^{-iu\kappa_2 \hat{x}} \rho_A(t) e^{iu\kappa_2 \hat{x}} L_2^\dagger \right). \tag{5.33}$$

In the end the establishment of the Master equation with consideration of the recoil comes down to adding a recoil term to each Lindblad operator

$$\begin{aligned} L_1 &\to L_1 e^{-iu\kappa_1 \hat{x}} \\ L_2 &\to L_2 e^{-iu\kappa_2 \hat{x}} \end{aligned} \tag{5.34}$$

and integrating over the z-component of the recoil momentum. Because the detuning is small in comparison to the frequency of the standing wave ω_L we may approximate

$$\kappa_1 = \kappa_2 = k_L \tag{5.35}$$

to simplify the simulations.

This addition of the recoil motion in equation (5.34) can be done at any moment, which is why for now we will go back to the original Lindblad operators (5.12) to simplify the formulas in the next step of our derivation, the adiabatic elimination.

5.3. Adiabatic Elimination of the Excited State

Let us now come back to the Master equation given in (5.10). The excited state has a very short life time, this means that atoms in this state will relax so frequently that we assume that this level is on average unpopulated. This is called adiabatic elimination. We shall derive now

from (5.10) the corresponding Master equation where the excited state has been eliminated using the effective Lindblad operator method introduced by Reiter and Sørensen [44]. The next three sections describe how this technique works.

For this part of the computation it is helpful to change to the Hamiltonian to a time independent frame to get rid of the time dependence of the interaction part and the excited subspace from the free evolution of the internal degree of freedom. We transform our Hamiltonian into the time-independent frame using the transformation

$$U = e^{-iH_T t} \tag{5.36}$$

with

$$H_T = (\omega_e - \omega_L)\,|1\rangle\langle 1| + (\omega_e - \omega_L)\,|2\rangle\langle 2| + \omega_e|e\rangle\langle e|. \tag{5.37}$$

This results in

$$H = U^\dagger\,(H - H_T)\,U \tag{5.38}$$

$$= \delta|1\rangle\langle 1| - \Delta|2\rangle\langle 2| + \frac{\Omega_1}{2}\cos(k_L\hat{x})\,(|1\rangle\langle e| + |e\rangle\langle 1|) \tag{5.39}$$

$$+ \frac{\Omega_2}{2}\cos(k_L\hat{x})\,(|2\rangle\langle e| + |e\rangle\langle 2|)\,. \tag{5.40}$$

5.3.1. Projection-Operator Method

Our Hamiltonian can be split into four parts describing the excited and ground subspaces

$$H = H_g + H_e + \underbrace{V_+ + V_-}_{V} \tag{5.41}$$

where

$$H_g = P_g H P_g = \delta|1\rangle\langle 1| - \Delta|2\rangle\langle 2| \tag{5.42}$$

$$H_e = P_e H P_e = 0 \tag{5.43}$$

$$V_+ = P_e H P_g = \frac{\Omega_1}{2}\cos(k_L\hat{x})|e\rangle\langle 1| + \frac{\Omega_2}{2}\cos(k_L\hat{x})|e\rangle\langle 2| \tag{5.44}$$

$$V_- = P_g H P_e = \frac{\Omega_1}{2}\cos(k_L\hat{x})|1\rangle\langle e| + \frac{\Omega_2}{2}\cos(k_L\hat{x})|2\rangle\langle e|. \tag{5.45}$$

P_g and P_e are the projection operators

$$P_g = |1\rangle\langle 1| + |2\rangle\langle 2| \tag{5.46}$$

$$P_e = |e\rangle\langle e|. \tag{5.47}$$

We will unite the unitary and dissipative dynamics of our system in a single non-Hermitian Hamiltonian H_{NH} in analogy to the one from the quantum jump picture [30]. In this case however only the dynamics from the excited subspace are included:

$$H_{NH} = H_e - \frac{i}{2} \sum_k L_k^\dagger L_k \tag{5.48}$$

$$= -i\frac{\gamma}{2}|e\rangle\langle e| \tag{5.49}$$

where γ is the total decay rate

$$\gamma = \gamma_1 + \gamma_2. \tag{5.50}$$

The Master equation can be rewritten in a reduced form by integrating parts of the dissipator together with the unitary dynamics in a non-hermitian Hamiltonian:

$$\dot{\rho}(t) = -i\left[(H_{NH} + H_g + V)\rho - \rho\left(H_{NH}^\dagger + H_g + V\right)\right] + \sum_k L_k \rho L_k^\dagger \tag{5.51}$$

this new Hamiltonian

$$H_{NH} + H_g + V \tag{5.52}$$

is sometimes referred to as effective Hamiltonian in the literature [41].

5.3.2. Transforming into a non-hermitian Interaction picture

In the next step we want to perform perturbation theory, for this we change to the interaction picture with the transformation

$$\mathcal{O}(t) = e^{-iH_g t}P_g + e^{-iH_{NH} t}P_e. \tag{5.53}$$

The non-hermiticity of the operator makes it so that the adjunct and the inverse do not match each other:

$$\mathcal{O}^\dagger(t) \neq \mathcal{O}^{-1}(t) \tag{5.54}$$

In this case the transformation rules for density operators, operators that are observables and those which are not differ from each other [45].

The transformation of a quantum state is:

$$|\tilde{\psi}\rangle = \mathcal{O}^{-1}(t)|\psi\rangle \tag{5.55}$$

From the transformation of the quantum state we can directly deduct the transformation of the density matrix:

$$\tilde{\rho}(t) = |\tilde{\psi}\rangle\langle\tilde{\psi}| \tag{5.56}$$

$$= \mathcal{O}^{-1}(t)|\psi\rangle\left(\mathcal{O}^{-1}(t)|\psi\rangle\right)^\dagger \tag{5.57}$$

$$= \mathcal{O}^{-1}(t)\rho\left(\mathcal{O}^{-1}(t)\right)^\dagger \tag{5.58}$$

For operators that are not density operators there are two possible ways to be transformed depending on whether it is an observable, a hermitian operator, or not.

In the case of an observable A, we can use the fact that the physics should not change by changing picture so the expectation value of an observable should stay the same:

$$\langle\tilde{\psi}(t)|\tilde{A}|\tilde{\psi}(t)\rangle \overset{!}{=} \langle\psi|A|\psi\rangle \tag{5.59}$$

$$= \langle\tilde{\psi}(t)|\mathcal{O}^\dagger(t)A\mathcal{O}(t)|\tilde{\psi}(t)\rangle \tag{5.60}$$

which means that

$$\tilde{A} = \mathcal{O}^\dagger(t)A\mathcal{O}(t). \tag{5.61}$$

The new equation of motion for the transformed state vector is:

$$\tilde{V}(t)|\tilde{\psi}\rangle = i\frac{d}{dt}|\tilde{\psi}\rangle \tag{5.62}$$

$$= i\frac{d}{dt}\left(\mathcal{O}^{-1}(t)|\psi\rangle\right) \tag{5.63}$$

$$= i\frac{d}{dt}\mathcal{O}^{-1}(t)|\psi\rangle + \mathcal{O}^{-1}(t)i\frac{d}{dt}|\psi\rangle \tag{5.64}$$

$$= -\mathcal{O}^{-1}(t)(H_g + H_{NH})|\psi\rangle + \mathcal{O}^{-1}(t)(H_g + H_{NH} + V)|\psi\rangle \tag{5.65}$$

$$= -\mathcal{O}^{-1}(t)(H_g + H_{NH})\mathcal{O}(t)|\tilde{\psi}\rangle + \mathcal{O}^{-1}(t)(H_g + H_{NH} + V)\mathcal{O}(t)|\tilde{\psi}\rangle \tag{5.66}$$

$$= \mathcal{O}^{-1}(t)V\mathcal{O}(t)|\tilde{\psi}\rangle \tag{5.67}$$

So non-hermitian operators O transform as

$$\tilde{O} = \mathcal{O}^{-1}(t)O\mathcal{O}(t). \tag{5.68}$$

Hence the for us relevant entities are transformed as follows:

$$\tilde{\rho}(t) = \mathcal{O}^{-1}(t)\rho\left(\mathcal{O}^{-1}(t)\right)^\dagger \tag{5.69}$$

$$\tilde{V}(t) = \mathcal{O}^{-1}(t)V\mathcal{O}(t) \tag{5.70}$$

$$\tilde{L}_i(t) = \mathcal{O}^{-1}(t)L_i\mathcal{O}(t) \tag{5.71}$$

5.3.3. Perturbation Theory

We expand the density operator perturbatively in order of the atom-field interactions, our small parameter.

$$\tilde{\rho}(t) = \tilde{\rho}^{(0)}(t) + \tilde{\rho}^{(1)}(t) + \tilde{\rho}^{(2)}(t) + \mathcal{O}(\tilde{V}^3) \tag{5.72}$$

$$\dot{\tilde{\rho}}^{(n)}(t) = -i\left(\tilde{V}(t)\tilde{\rho}^{(n-1)}(t) - \tilde{\rho}^{(n-1)}(t)\tilde{V}^\dagger(t)\right) + \sum_k \tilde{L}_k(t)\tilde{\rho}^{(n)}(t)\tilde{L}_k^\dagger(t) \tag{5.73}$$

The adiabatic elimination takes place in two steps. First we assume that in the beginning there are no excited atoms, so that $\tilde{\rho}^{(n)}(t)$ for $n \leq 1$ contains no excited part $\tilde{\rho}_{ee}^{(n)}(t)$. This assumption is safe since the atoms are only getting excited by the standing-wave laser during the kick and decay rapidly so that earlier excitations should have relaxed.

$$\dot{\tilde{\rho}}^{(0)}(t) = 0 \tag{5.74}$$

$$\dot{\tilde{\rho}}^{(1)}(t) = -i\left(\tilde{V}(t)\tilde{\rho}^{(0)}(t) - \tilde{\rho}^{(0)}(t)\tilde{V}^\dagger(t)\right) \tag{5.75}$$

$$\dot{\tilde{\rho}}^{(2)}(t) = -i\left(\tilde{V}(t)\tilde{\rho}^{(1)}(t) - \tilde{\rho}^{(1)}(t)\tilde{V}^\dagger(t)\right) + \sum_k \tilde{L}_k(t)\tilde{\rho}^{(2)}(t)\tilde{L}_k^\dagger(t) \tag{5.76}$$

The evolution of the excited and the ground states is separated by means of projection operators.

$$P_g\dot{\tilde{\rho}}^{(0)}(t)P_g = P_g\dot{\tilde{\rho}}^{(1)}(t)P_g = 0 \tag{5.77}$$

$$P_g\dot{\tilde{\rho}}^{(2)}(t)P_g = -iP_g\left(\tilde{V}(t)\tilde{\rho}^{(1)}(t) - \tilde{\rho}^{(1)}(t)\tilde{V}^\dagger(t)\right)P_g + \sum_k \tilde{L}_k(t)\tilde{\rho}^{(2)}(t)\tilde{L}_k^\dagger(t) \tag{5.78}$$

$$P_e\dot{\tilde{\rho}}^{(0)}(t)P_e = P_e\dot{\tilde{\rho}}^{(1)}(t)P_e = 0 \tag{5.79}$$

$$P_e\dot{\tilde{\rho}}^{(2)}(t)P_e = -iP_e\left(\tilde{V}(t)\tilde{\rho}^{(1)}(t) - \tilde{\rho}^{(1)}(t)\tilde{V}^\dagger(t)\right)P_e \tag{5.80}$$

In the second step of the adiabatic elimination we say that the change in population of the excited state that solely depends on (5.80) is infinitesimal

$$P_e\dot{\tilde{\rho}}^{(2)}(t)P_e = 0. \tag{5.81}$$

Then the evolution of our system is then described only by the time evolution in the subspace of ground states:

$$P_g\dot{\tilde{\rho}}^{(2)}(t)P_g = -iP_g\left(\tilde{V}(t)\tilde{\rho}^{(1)}(t) - \tilde{\rho}^{(1)}(t)\tilde{V}^\dagger(t)\right)P_g + \sum_k \tilde{L}_k(t)\tilde{\rho}^{(2)}(t)\tilde{L}_k^\dagger(t) \tag{5.82}$$

No initial excitation comes down to removing terms of the following form:

$$P_g\tilde{V}(t)\tilde{\rho}^{(0)}(t)\tilde{V}(t)P_g = P_g\tilde{V}^\dagger(t)\tilde{\rho}^{(0)}(t)\tilde{V}^\dagger(t)P_g = P_e\tilde{\rho}^{(0)}P_e = 0 \tag{5.83}$$

It remains:

$$P_g\dot{\tilde{\rho}}^{(2)}(t)P_g = \underbrace{-P_g\tilde{V}(t)\int_0^t dt'\tilde{V}(t')\tilde{\rho}^{(0)}(t')P_g}_{I_1} - P_g\int_0^t dt'\tilde{\rho}^{(0)}(t')\tilde{V}^\dagger(t')\tilde{V}^\dagger(t)P_g \tag{5.84}$$

$$+ P_g\sum_k \tilde{L}_k(t)\,P_e\underbrace{\int_0^t dt'\int_0^{t'} dt''\tilde{V}(t')\tilde{\rho}^{(0)}(t'')\tilde{V}^\dagger(t'')P_e}_{I_2}\,\tilde{L}_k^\dagger(t)P_g \tag{5.85}$$

$$+ P_g\sum_k \tilde{L}_k(t)P_e\int_0^t dt'\int_0^{t'} dt''\tilde{V}(t'')\tilde{\rho}^{(0)}(t'')\tilde{V}^\dagger(t')P_e\tilde{L}_k^\dagger(t)P_g \tag{5.86}$$

The terms after I_1 and I_2 just correspond to their hermitian conjugate.

We transform back to the Schrödinger picture using the transformation equations (5.69). The $\mathcal{O}(t)$ cancel each other out in pairwise fashion:

$$\mathcal{O}(t)P_g\dot{\tilde{\rho}}^{(2)}(t)P_g\mathcal{O}^\dagger(t) = P_g\dot{\rho}^{(2)}(t)P_g \tag{5.87}$$

$$\mathcal{O}(t)I_1\mathcal{O}^\dagger(t) = iP_gV_-\sum_l (H_{NH} - E_l)^{-1} V_+^{(l)}\rho^{(0)} \tag{5.88}$$

$$\mathcal{O}(t)P_g\sum_k \tilde{L}_k(t)I_2\tilde{L}_k^\dagger(t)P_g\mathcal{O}^\dagger(t) = \sum_k L_k\sum_l \frac{1}{H_{NH} - E_l}V_+^{(l)}\rho^{(0)} \tag{5.89}$$

$$\cdot\sum_{l'} V_-^{(l')}\frac{1}{H_{NH}^\dagger - E_{l'}}L_k^\dagger \tag{5.90}$$

We have then after transforming back to the Schrödinger picture the following equivalences:

$$V_-\sum_l \frac{1}{H_{NH} - E_l}V_+^{(l)}\rho^{(0)} = -i\left(H_{\text{eff}} - \frac{i}{2}\sum_l L_{\text{eff},l}^\dagger L_{\text{eff},l}\right)\rho^{(0)} \tag{5.91}$$

and

$$\sum_l L_l\frac{1}{H_{NH} - E_l}V_+\rho^{(0)}V_-\frac{1}{H_{NH}^\dagger - E_l}L_l^\dagger = \sum_l L_{\text{eff},l}\rho^{(0)}L_{\text{eff},l}^\dagger \tag{5.92}$$

In our case:

$$\frac{1}{H_{NH} - E_1} = \frac{1}{H_{NH} - \delta} \tag{5.93}$$

$$\frac{1}{H_{NH} - E_2} = \frac{1}{H_{NH} + \Delta} \tag{5.94}$$

5.3.4. Result

Now we can compute the effective Hamiltonian and the effective Lindblad operators.

$$H_{\text{eff}} = -\frac{1}{2}\left[V_- \sum_l \frac{1}{H_{NH} - E_l} V_+^{(l)} + V_+ \sum_l \frac{1}{H_{NH}^\dagger - E_l} V_-^{(l)} \right] + H_g \tag{5.95}$$

$$= \left(\delta + \frac{\delta \Omega_2^2 \cos^2(k_L \hat{X})}{4\delta^2 + \gamma^2} \right) |1\rangle\langle 1| + \left(-\Delta - \frac{\Delta \Omega_1^2 \cos^2(k_L \hat{X})}{4\Delta^2 + \gamma^2} \right) |2\rangle\langle 2| \tag{5.96}$$

$$+ \frac{(\Delta - \delta)\Omega_1\Omega_2 \cos^2(k_L \hat{X})}{8(\Delta - i\frac{\gamma}{2})(-\delta - i\frac{\gamma}{2})} |2\rangle\langle 1| + \frac{(\Delta - \delta)\Omega_1\Omega_2 \cos^2(k_L \hat{X})}{8(\Delta + i\frac{\gamma}{2})(-\delta + i\frac{\gamma}{2})} |1\rangle\langle 2| \tag{5.97}$$

The first thing to remark is that in the limit of vanishing spontaneous emission $\gamma \to 0$ we recover the Hamiltonian (3.19) derived with help of the effective Hamiltonian theory. Here we also get an effective coupling between the two ground state but its vanishingly small as it scales with the difference of the detuning and in the main case of equal detuning it disappears completely.

$$H_{\text{eff}} = \left(\delta + \frac{\delta \Omega_2^2 \cos^2(k_L \hat{x})}{4\delta^2 + \gamma^2} \right) |1\rangle\langle 1| + \left(-\Delta - \frac{\Delta \Omega_1^2 \cos^2(k_L \hat{x})}{4\Delta^2 + \gamma^2} \right) |2\rangle\langle 2| \tag{5.98}$$

Note that in the effective Hamiltonian theory in section 3.2 only the atom-field interaction part of the Hamiltonian is treated which is why we do not have the level structure of the internal levels as we have here.

Our new effective Lindblad operators

$$L_{\text{eff},1} = L_1 \left(\frac{1}{H_{NH} - E_1} V_+^{(1)} + \frac{1}{H_{NH} - E_2} V_+^{(2)} \right) \tag{5.99}$$

$$= \sqrt{\gamma_1} \cos(k_L \hat{x}) \left[\frac{\Omega_1}{2(-\delta - \frac{i\gamma}{2})} |1\rangle\langle 1| + \frac{\Omega_2}{2(\Delta - \frac{i\gamma}{2})} |1\rangle\langle 2| \right] \tag{5.100}$$

$$L_{\text{eff},2} = L_2 \left(\frac{1}{H_{NH} - E_1} V_+^{(1)} + \frac{1}{H_{NH} - E_2} V_+^{(2)} \right) \tag{5.101}$$

$$= \sqrt{\gamma_2} \cos(k_L \hat{x}) \left[\frac{\Omega_1}{2(-\delta - \frac{i\gamma}{2})} |2\rangle\langle 1| + \frac{\Omega_2}{2(\Delta - \frac{i\gamma}{2})} |2\rangle\langle 2| \right] \tag{5.102}$$

are now bipartite. Since the excited level was adiabatically eliminated they no longer describe just a decay from the excited state to one of the ground levels but also the excitation process, the absorption of a photon from the standing-wave laser, that just precedes the spontaneous emission. In [46] the cosinusoidal position dependence of the Lindblad operators is interpreted as the fact that spontaneous emission is the most abundant where the standing wave is the strongest because the stronger the standing wave at a point the more atoms are excited. We shall construe it as the recoil that comes from absorbing a photon and has to be evaluated

as a coherent momentum shift by plus and minus half a momentum unit for the two photon directions in the standing wave.

$$\cos(k_L \hat{x}) = \frac{e^{ik_L \hat{x}} + e^{-ik_L \hat{x}}}{2}.$$

(5.103)

After its application the quasimomentum has to be adjusted as described in section 2.3.

Let us now reintroduce the recoil motion that we derived prior to that and separate the dynamics of the external and the internal degree of freedom in the Lindbladians:

$$
\begin{aligned}
L_{\text{eff},i} &= \sqrt{\gamma_i} L_{\text{eff},i,\text{ext}} L_{\text{eff},i,\text{int}} \\
L_{\text{eff},1,\text{ext}} &= \cos(k_L \hat{x}) e^{iuk_L \hat{x}} \\
L_{\text{eff},1,\text{int}} &= \left[\frac{\Omega_1}{2(-\delta - \frac{i\gamma}{2})} |1\rangle\langle 1| + \frac{\Omega_2}{2(\Delta - \frac{i\gamma}{2})} |1\rangle\langle 2| \right] \\
L_{\text{eff},2,\text{ext}} &= \cos(k_L \hat{x}) e^{iuk_L \hat{x}} \\
L_{\text{eff},2,\text{int}} &= \left[\frac{\Omega_1}{2(-\delta - \frac{i\gamma}{2})} |2\rangle\langle 1| + \frac{\Omega_2}{2(\Delta - \frac{i\gamma}{2})} |2\rangle\langle 2| \right]
\end{aligned}
$$

(5.104)

Then the final result for the Master equation in natural units

$$
\begin{aligned}
\dot{\rho}_A(t) = &-i \left[H_{\text{eff}}, \rho_A(t) \right] \\
&- \frac{\gamma_1}{2} \left(L_{\text{eff},1,\text{int}}^\dagger L_{\text{eff},1,\text{int}} \cos^2\left(\frac{\theta}{2}\right) \rho_A(t) + \rho_A(t) \cos^2\left(\frac{\theta}{2}\right) L_{\text{eff},1,\text{int}}^\dagger L_{\text{eff},1,\text{int}} \right. \\
&\left. - 2 \int_{-1}^1 du\, \Phi(u) L_{\text{eff},1,\text{int}} e^{-iu\frac{\theta}{2}} \cos\left(\frac{\theta}{2}\right) \rho_A(t) \cos\left(\frac{\theta}{2}\right) e^{iu\frac{\theta}{2}} L_{\text{eff},1,\text{int}}^\dagger \right) \\
&- \frac{\gamma_2}{2} \left(L_{\text{eff},2,\text{int}}^\dagger L_{\text{eff},2,\text{int}} \cos^2\left(\frac{\theta}{2}\right) \rho_A(t) + \rho_A(t) \cos^2\left(\frac{\theta}{2}\right) L_{\text{eff},2,\text{int}}^\dagger L_{\text{eff},2,\text{int}} \right. \\
&\left. - 2 \int_{-1}^1 du\, \Phi(u) L_{\text{eff},2,\text{int}} e^{-iu\frac{\theta}{2}} \cos\left(\frac{\theta}{2}\right) \rho_A(t) \cos\left(\frac{\theta}{2}\right) e^{iu\frac{\theta}{2}} L_{\text{eff},2,\text{int}}^\dagger \right)
\end{aligned}
$$

(5.105)

is similar to the results derived for a simple kicked rotor model [46, 47]. The major difference being that here there is one more dissipator and the Lindblad operator are more complicated which can easily be explained by the additional ground state. The other difference is that we also account for the finite width of the pulse duration, which is why we do not have a discrete summation like in [46]. This also allows for multiple decay processes during one kick.

5.4. Effective Kick Strength

The new effective Hamiltonian in equation (5.95) has now a γ-dependence in its denominator that will transmit to the kick strength and the light shift phase. Let us perform the same calculation as we performed with the effective Hamiltonian without spontaneous emission in section 3.2:

$$H_{\text{eff}} = \frac{\delta \Omega_2^2 \cos^2(k_L \hat{x})}{4\delta^2 + \gamma^2} |1\rangle\langle 1| - \frac{\Delta \Omega_1^2 \cos^2(k_L \hat{x})}{4\Delta^2 + \gamma^2} |2\rangle\langle 2| \tag{5.106}$$

$$= \frac{4\delta^2}{4\delta^2 + \gamma^2} \frac{\Omega_2^2 \cos^2(k_L \hat{x})}{4\delta} |1\rangle\langle 1| - \frac{4\Delta^2}{4\Delta^2 + \gamma^2} \frac{\Omega_1^2 \cos^2(k_L \hat{x})}{4\Delta} |2\rangle\langle 2| \tag{5.107}$$

$$= \frac{1}{1 + \frac{\gamma^2}{4\delta^2}} \left(\frac{\Omega_1^2 \cos(2k_L \hat{x})}{8\delta} + \frac{\Omega_1^2}{8\delta} \right) |1\rangle\langle 1| \tag{5.108}$$

$$- \frac{1}{1 + \frac{\gamma^2}{4\Delta^2}} \left(\frac{\Omega_2^2 \cos(2k_L \hat{x})}{8\Delta} + \frac{\Omega_2^2}{8\Delta} \right) |2\rangle\langle 2| \tag{5.109}$$

which leads to a rescaled kick strength

$$k_{\text{eff}} = k \frac{1}{1 + \frac{\gamma^2}{4\Delta^2}}. \tag{5.110}$$

For typical spontaneous emission rates we have $\gamma \ll \Delta$ and the rescaling factor is near unity and we can safely just take

$$k_{\text{eff}} \approx k. \tag{5.111}$$

5.5. Numerical Results

To complete this chapter, let us finish by showing some preliminary numerical results of the spontaneous emission. The spontaneous emission rate γ here is given as a decay probability per kick for better readability.
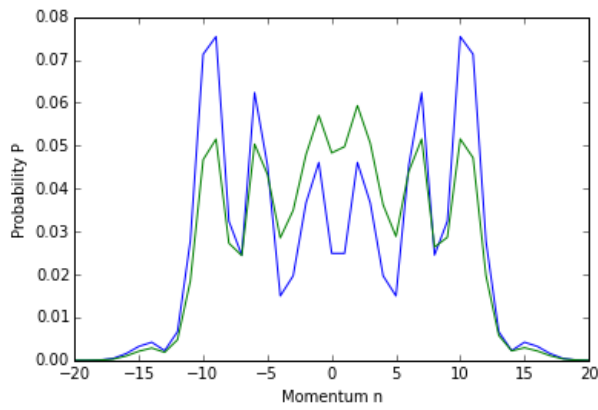
$T = 10$ and $\gamma = 0.05$
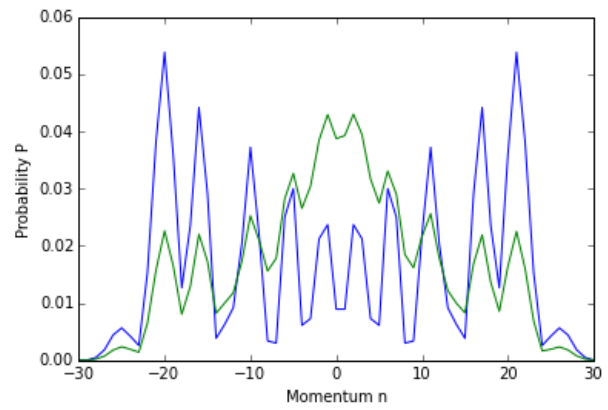
$T = 20$ and $\gamma = 0.05$
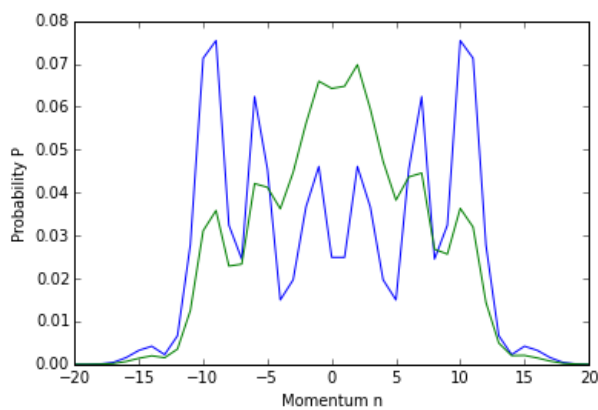
$T = 10$ and $\gamma = 0.1$
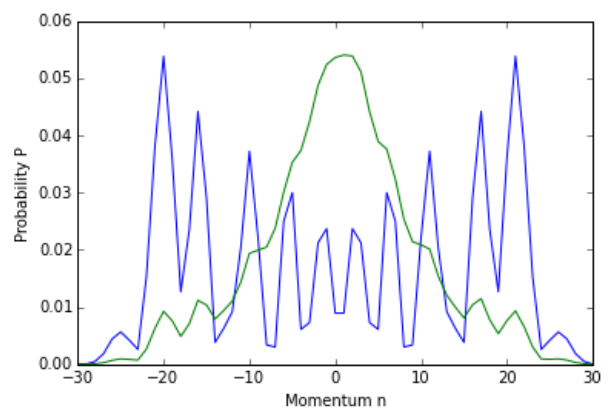
$T = 20$ and $\gamma = 0.1$

Figure 5.1.: Momentum distribution with kick strength $k = 2$, 10000 quantum trajectories, kick number T and spontaneous emission rates γ. Ideal walks (blue) and decoherent walks (green).

In the limit of large times, the quantum feature interference disappears completely as can be seen in the next plot. The momentum distribution does not seem to trend towards a Gaussian but rather localize.
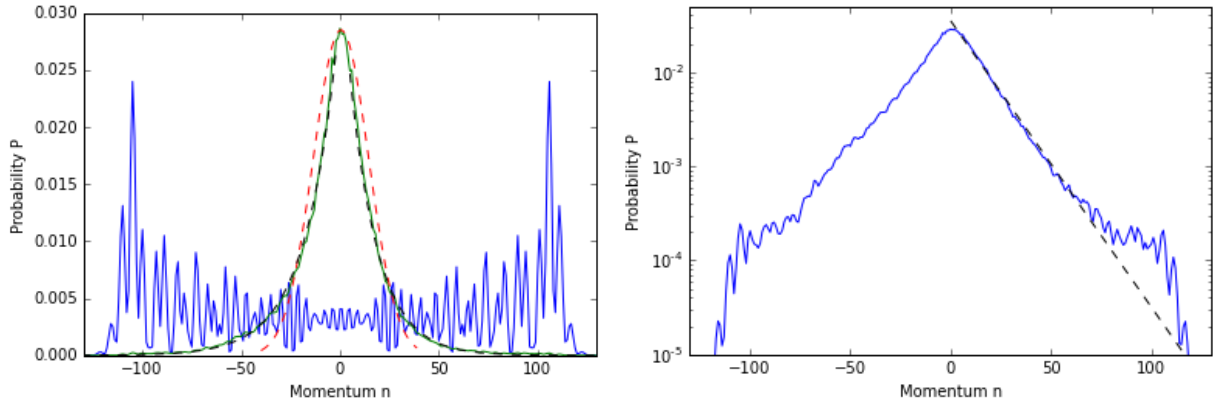
Figure 5.2.: Momentum distribution with kick strength $k = 2$, 1000 quantum trajectories, kick number T and spontaneous emission rates $\gamma = 0.05$. Ideal walk (blue), decoherent walk (green), Gaussian approximation (red) and exponential approximation (black). And just the decoherent walk with exponential fit in semi-logarithmic plot.

To reduce the computation time we can also approximate the cosine by its standard deviation

$$\cos(k_L \hat{x}) \approx \frac{1}{\sqrt{2}}, \tag{5.112}$$

which leads to results that are in line with the coherent momentum shift.
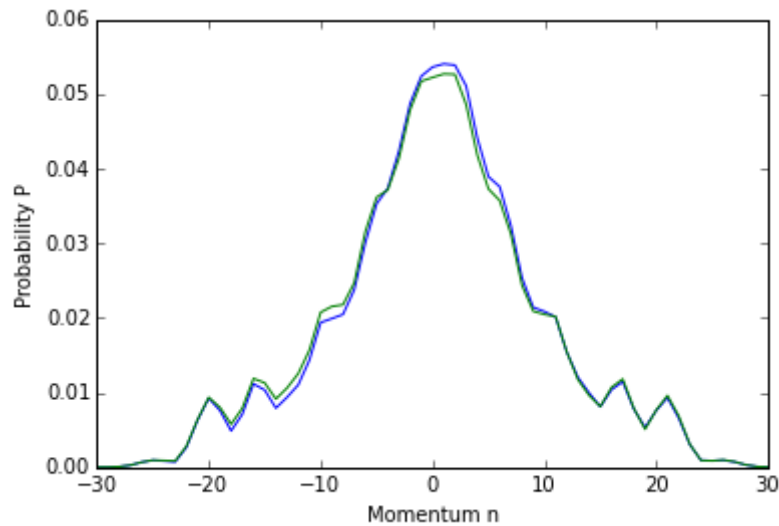
Figure 5.3.: Comparative plot of the momentum distributions of quantum walk with kick strength $k = 2$, kick numbers $T = 20$, spontaneous emission probability per kick of $\gamma = 0.1$ and 10000 quantum trajectories. In one case (green) the cosine has been approximated in the second (blue) not.

Conclusion

Summary

In the end this thesis represents a preliminary investigation of the proposed quantum walk scheme. Let us briefly summarize our findings:

We could analytically solve the time evolution of the walk procedure proposed in the paper. Furthermore we inspected the dependence of the walk on its two main parameters the kick strength and the kick number. We observed that the first one had the same effect on the walk as it has on normal quantum walk in position space, it spreads the distribution and makes the standard deviation grow linearly. The kick strength on the other hand showed disruptive influence on the walk especially for too great amplitudes. In consequence we had to restrict it to a small segment around the ideal value of $k = 2$ to have a 'good' quantum walk.

We treated the system from a quantum optical point of view and derived with help of the effective Hamiltonian theory the time averaged dynamics of the atom during the kick. Here we could show that the proposed experimental implementation did not exactly correspond to the walk described in the paper. The effective two-level nature of the system introduces a relative phase between the two ground states that had to be compensated to obtain the proposed quantum walk.

Finally we completed the description of the dynamics of the atom during the kick by creating a full description, taking into account the internal and external dynamics, by adding spontaneous emission as a decoherence effect.

Outlook

To finish of we shall mentions some aspect that we have not treated yet but that might be interesting to pave the avenue for future investigations.

In the theoretical preliminaries we presented how more complex quantum ratchets could lead to less dispersion or a more directed motion. The big difference from our walk to typical ones is that we do not do a discrete step of one momentum step to the right or the left but rather

have this change of the average momentum. The analytical solution for the momentum distribution can actually be very easily expanded to more complex ratchets as long as the relative phase between momentum classes that differ by $\Delta n = 1$ is either $\frac{\pi}{2}$ or $-\frac{\pi}{2}$.

The kick strength has until now always be assumed constant along a kick sequence. But experimentally though the intensity of the laser on which it depends tends to drift if one measures over a long period. Additionally atoms feel different intensities depending on whether there are in the centre or the edge of the laser beam because of its non-uniform profile. Different kick strengths would also mean different relative phases between the two internal levels which would make the compensation more difficult, as discussed in section 3.3. A thorough analysis would give us the opportunity to connect this work with previous investigations concerning the steering of classical random walks by way of varying the kick strength [48].

As for the steering of random walks with kicked ultra cold atoms another experimental uncertainty is the kick period, one needs to check what happens to the quantum walk for small detunings from quantum resonance

One should also consider a noise in the coin, small random phases in the mixing, although experimentally this seems to be the best controlled factor so it is unlikely that it plays a big role in the sum of all decoherence effects.

One should further investigate why the walk does not trend towards a normal distribution. Localization has been observed in quantum walks where the coin was position dependent [49].

Appendix

A. Bessel Functions of the first kind

Bessel functions [50] will make a recurring appearance when one is working the quantum kicked rotor model. This appendix aims to briefly introduce their concept and present the important formulas that we will use through our calculations. Bessel functions of the first kind are solutions to the Bessel differential equation:

$$z^2 \frac{d^2 f}{dz^2} + z\frac{df}{dz} + (z^2 - n^2)f = 0 \tag{A.1}$$

and are defined as

$$J_n(z) = \sum_{r=0}^{\infty} \frac{(-1)^r (\frac{z}{2})^{2r+n}}{\Gamma(n+r+1)r!} \tag{A.2}$$

where $\Gamma(x)$ represents the Gamma function. For integer-valued indexes of the Bessel functions the following relationships holds:

$$J_{-n}(z) = (-1)^n J_n(z) = J_n(-z) \tag{A.3}$$

The reason for the aforementioned recurrence of the Bessel function is the so-called Jacobi-Anger expansion in which one can write what in our work is the kick part of the Floquet operator as an expansion of Bessel function.

$$e^{iz\cos\theta} = \sum_{m=-\infty}^{\infty} i^m J_m(z)e^{im\theta} \tag{A.4}$$

From here we can execute the θ-integration and get an integral representation of the Bessel function. This will be used to derive the momentum distribution.

$$\int_0^{2\pi} e^{in\theta} e^{iz\cos\theta} d\theta = 2\pi i^n J_n(z) \tag{A.5}$$

B. Calculations concerning the momentum distribution

Proof that the matrix entries are recursive polynomials

Before we embark on the actual proof of the recursion we will advance two small calculations that we show to be useful in the during the proof.

$$z^2 - \tilde{z}^2 = e^{-2ik\cos\hat{\theta}} + 2 + e^{2ik\cos\hat{\theta}} - (e^{-2ik\cos\hat{\theta}} - 2 + e^{2ik\cos\hat{\theta}})$$

$$= 4$$

$$
\begin{aligned}
(z\tilde{z} + z^2 - 8)(z - \tilde{z}) &= \Big((e^{-ik\cos\hat{\theta}} + e^{ik\cos\hat{\theta}})(e^{-ik\cos\hat{\theta}} - e^{ik\cos\hat{\theta}}) \\
&\quad + (e^{-ik\cos\hat{\theta}} + e^{ik\cos\hat{\theta}})^2 - 8 \Big) \\
&\quad \cdot \Big((e^{-ik\cos\hat{\theta}} + e^{ik\cos\hat{\theta}}) - (e^{-ik\cos\hat{\theta}} - e^{ik\cos\hat{\theta}}) \Big) \\
&= (e^{-2ik\cos\hat{\theta}} - e^{2ik\cos\hat{\theta}} + e^{-2ik\cos\hat{\theta}} + 2 + e^{2ik\cos\hat{\theta}} - 8)2e^{ik\cos\hat{\theta}} \\
&= 4(e^{-ik\cos\hat{\theta}} - 3e^{ik\cos\hat{\theta}}) \\
&= 4\Big(2(e^{-ik\cos\hat{\theta}} - e^{ik\cos\hat{\theta}}) - (e^{-ik\cos\hat{\theta}} + e^{ik\cos\hat{\theta}}) \Big) \\
&= 4(2\tilde{z} - z)
\end{aligned}
$$

The hypothesis, that the matrix entries follow the polynomial form as said in equation (4.7) is shown via mathematical induction. The base case is trivially true and now we show the inductive step, that if the N-th matrix entries $A_1^{(N)}$ and $A_2^{(N)}$ have the polynomial form so will $A_1^{(N+1)}$ and $A_2^{(N+1)}$:

$$A_1^{(N+1)} = e^{-ik\cos\hat\theta}\left(A_1^{(N)} + iA_2^{(N)}\right)$$

$$= e^{-ik\cos\hat\theta}\left(e^{-ik\cos\hat\theta}p_1^{(N)} - e^{ik\cos\hat\theta}p_2^{(N)}\right)$$

$$= e^{-ik\cos\hat\theta}\left(\frac{z+\tilde z}{2}p_1^{(N)} - \frac{z-\tilde z}{2}p_2^{(N)}\right)$$

$$= e^{-ik\cos\hat\theta}\left(zp_1^{(N)} - \frac{z-\tilde z}{2}(p_1^{(N)} + p_2^{(N)})\right)$$

$$= e^{-ik\cos\hat\theta}\left[zp_1^{(N)} - \frac{z-\tilde z}{2}\left(\frac{1}{2}(1 + \frac{2\tilde z - z}{\sqrt{z^2-8}})(\frac{z+\sqrt{z^2-8}}{2})^N + \frac{1}{2}(1 - \frac{2\tilde z - z}{\sqrt{z^2-8}})(\frac{z-\sqrt{z^2-8}}{2})^N \right.\right.$$

$$\left.\left. + \frac{1}{2}(1 + \frac{z}{\sqrt{z^2-8}})(\frac{z+\sqrt{z^2-8}}{2})^N + \frac{1}{2}(1 - \frac{z}{\sqrt{z^2-8}})(\frac{z-\sqrt{z^2-8}}{2})^N\right)\right]$$

$$= e^{-ik\cos\hat\theta}\left[zp_1^{(N)} - \frac{z-\tilde z}{2}\left(\frac{1}{2}(2 + \frac{2\tilde z}{\sqrt{z^2-8}})(\frac{z+\sqrt{z^2-8}}{2})^N \right.\right.$$

$$\left.\left. + \frac{1}{2}(2 - \frac{2\tilde z}{\sqrt{z^2-8}})(\frac{z-\sqrt{z^2-8}}{2})^N\right)\right]$$

$$= e^{-ik\cos\hat\theta}\left[zp_1^{(N)} - \left((\frac{z-\tilde z}{2} + \frac{\tilde z(z-\tilde z)}{2\sqrt{z^2-8}})(\frac{z+\sqrt{z^2-8}}{2})^N \right.\right.$$

$$\left.\left. + (\frac{z-\tilde z}{2} - \frac{\tilde z(z-\tilde z)}{2\sqrt{z^2-8}})(\frac{z-\sqrt{z^2-8}}{2})^N\right)\right]$$

$$= e^{-ik\cos\hat\theta}\left[zp_1^{(N)} - \left((\frac{(z-\tilde z)z}{4} + \frac{z\tilde z(z-\tilde z)}{4\sqrt{z^2-8}} + \frac{\sqrt{z^2-8}(z-\tilde z)}{4} + \frac{\tilde z(z-\tilde z)}{4})(\frac{z+\sqrt{z^2-8}}{2})^{N-1} \right.\right.$$

$$\left.\left. + (\frac{(z-\tilde z)z}{4} - \frac{z\tilde z(z-\tilde z)}{4\sqrt{z^2-8}} - \frac{\sqrt{z^2-8}(z-\tilde z)}{4} + \frac{\tilde z(z-\tilde z)}{4})(\frac{z-\sqrt{z^2-8}}{2})^{N-1}\right)\right]$$

$$= e^{-ik\cos\hat\theta}\left[zp_1^{(N)} - \left((\frac{z^2-\tilde z^2}{4} + \frac{(z\tilde z + z^2 - 8)(z-\tilde z)}{4\sqrt{z^2-8}})(\frac{z+\sqrt{z^2-8}}{2})^{N-1} \right.\right.$$

$$\left.\left. + (\frac{z^2-\tilde z^2}{4} - \frac{(z\tilde z + z^2 - 8)(z-\tilde z)}{4\sqrt{z^2-8}})(\frac{z-\sqrt{z^2-8}}{2})^{N-1}\right)\right]$$

$$= e^{-ik\cos\hat\theta}\left[zp_1^{(N)} - \left((1 + \frac{2\tilde z - z}{\sqrt{z^2-8}})(\frac{z+\sqrt{z^2-8}}{2})^{N-1} + (1 - \frac{2\tilde z - z}{\sqrt{z^2-8}})(\frac{z-\sqrt{z^2-8}}{2})^{N-1}\right)\right]$$

$$= e^{-ik\cos\hat\theta}(zp_1^{(N)} - 2p_1^{(N-1)})$$

$$= e^{-ik\cos\hat\theta}p_1^{(N+1)}$$

And likewise for the second matrix entry:

$$
\begin{aligned}
A_2^{(N+1)} &= e^{ik\cos\hat\theta}\left(iA_1^{(N)} + A_2^{(N)}\right) \\
&= e^{ik\cos\hat\theta}\left(ie^{-ik\cos\hat\theta}p_1^{(N)} + ie^{ik\cos\hat\theta}p_2^{(N)}\right) \\
&= ie^{ik\cos\hat\theta}\left(\frac{z+\tilde z}{2}p_1^{(N)} + \frac{z-\tilde z}{2}p_2^{(N)}\right) \\
&= ie^{ik\cos\hat\theta}\left(zp_2^{(N)} - \frac{z+\tilde z}{2}(-p_1^{(N)} + p_2^{(N)})\right) \\
&= ie^{ik\cos\hat\theta}\Bigg[zp_2^{(N)} - \frac{z+\tilde z}{2}\Bigg(-\frac{1}{2}(1 + \frac{2\tilde z - z}{\sqrt{z^2-8}})(\frac{z+\sqrt{z^2-8}}{2})^N \\
&\quad -\frac{1}{2}(1 - \frac{2\tilde z - z}{\sqrt{z^2-8}})(\frac{z-\sqrt{z^2-8}}{2})^N \\
&\quad +\frac{1}{2}(1 + \frac{z}{\sqrt{z^2-8}})(\frac{z+\sqrt{z^2-8}}{2})^N + \frac{1}{2}(1 - \frac{z}{\sqrt{z^2-8}})(\frac{z-\sqrt{z^2-8}}{2})^N\Bigg)\Bigg] \\
&= ie^{ik\cos\hat\theta}\Bigg[zp_2^{(N)} - \frac{z+\tilde z}{2}\Bigg(\frac{1}{2}(\frac{2(-\tilde z + z)}{\sqrt{z^2-8}})(\frac{z+\sqrt{z^2-8}}{2})^N + \frac{1}{2}(\frac{2(\tilde z - z)}{\sqrt{z^2-8}})(\frac{z-\sqrt{z^2-8}}{2})^N\Bigg)\Bigg] \\
&= ie^{ik\cos\hat\theta}\Bigg[zp_2^{(N)} - \Bigg(\frac{z^2 - \tilde z^2}{2\sqrt{z^2-8}}(\frac{z+\sqrt{z^2-8}}{2})^N + \frac{\tilde z^2 - z^2}{2\sqrt{z^2-8}}(\frac{z-\sqrt{z^2-8}}{2})^N\Bigg)\Bigg] \\
&= ie^{ik\cos\hat\theta}\Bigg[zp_2^{(N)} - \Bigg((\frac{z(z^2 - \tilde z^2)}{4\sqrt{z^2-8}} + \frac{z^2 - \tilde z^2}{4})(\frac{z+\sqrt{z^2-8}}{2})^{N-1} \\
&\quad + (\frac{z(-z^2 + \tilde z^2)}{4\sqrt{z^2-8}} - \frac{-z^2 + \tilde z^2}{4})(\frac{z-\sqrt{z^2-8}}{2})^{N-1}\Bigg)\Bigg] \\
&= ie^{ik\cos\hat\theta}\Bigg[zp_2^{(N)} - \Bigg((1 + \frac{z}{\sqrt{z^2-8}})(\frac{z+\sqrt{z^2-8}}{2})^{N-1} + (1 - \frac{z}{\sqrt{z^2-8}})(\frac{z-\sqrt{z^2-8}}{2})^{N-1}\Bigg)\Bigg] \\
&= ie^{ik\cos\hat\theta}(zp_2^{(N)} - 2p_2^{(N-1)}) \\
&= ie^{ik\cos\hat\theta}p_2^{(N+1)}
\end{aligned}
$$

Rewriting of the polynomials into a more accessible form

$$
\begin{aligned}
p_1^{(N)}(z) &= \frac{1}{2}\left(1 + \frac{2\tilde{z} - z}{\sqrt{z^2 - 8}}\right)\left(\frac{z + \sqrt{z^2 - 8}}{2}\right)^N + \frac{1}{2}\left(1 - \frac{2\tilde{z} - z}{\sqrt{z^2 - 8}}\right)\left(\frac{z - \sqrt{z^2 - 8}}{2}\right)^N \\
&= \frac{1}{2^{N+1}}\left[\left(1 + \frac{2\tilde{z} - z}{\sqrt{z^2 - 8}}\right)(z + \sqrt{z^2 - 8})^N + \left(1 - \frac{2\tilde{z} - z}{\sqrt{z^2 - 8}}\right)(z - \sqrt{z^2 - 8})^N\right] \\
&= \frac{1}{2^{N+1}}\left[(z + \sqrt{z^2 - 8})^N + (z - \sqrt{z^2 - 8})^N + \frac{2\tilde{z} - z}{\sqrt{z^2 - 8}}\left((z + \sqrt{z^2 - 8})^N - (z - \sqrt{z^2 - 8})^N\right)\right] \\
&= \frac{1}{2^{N+1}}\left[\sum_{j=0}^{N}\binom{N}{j}z^{N-j}(\sqrt{z^2 - 8})^j + \sum_{j=0}^{N}\binom{N}{j}z^{N-j}(-\sqrt{z^2 - 8})^j\right. \\
&\quad \left. + \frac{2\tilde{z} - z}{\sqrt{z^2 - 8}}\left(\sum_{j=0}^{N}\binom{N}{j}z^{N-j}(\sqrt{z^2 - 8})^j - \sum_{j=0}^{N}\binom{N}{j}z^{N-j}(-\sqrt{z^2 - 8})^j\right)\right] \\
&= \frac{1}{2^{N}}\left[\sum_{j=0}^{\frac{N}{2}}\binom{N}{2j}z^{N-2j}(z^2 - 8)^j + \frac{2\tilde{z} - z}{\sqrt{z^2 - 8}}\sum_{j=0}^{\frac{N}{2}}\binom{N}{2j + 1}z^{N-2j-1}(\sqrt{z^2 - 8})^{2j+1}\right] \\
&= \frac{1}{2^{N}}\left[\sum_{j=0}^{\frac{N}{2}}\left(\binom{N}{2j} - \binom{N}{2j + 1}\right)z^{N-2j}(z^2 - 8)^j + 2\sum_{j=0}^{\frac{N}{2}}\binom{N}{2j + 1}\tilde{z}z^{N-2j-1}(z^2 - 8)^j\right] \\
&= \frac{1}{2^{N}}\left[\sum_{j=0}^{\frac{N}{2}}\sum_{m=0}^{j}\sum_{l=0}^{N-2m}\left(\binom{N}{2j} - \binom{N}{2j + 1}\right)\binom{j}{m}\binom{N - 2m}{l}e^{ik\cos\hat{\theta}(N-2m-2l)}(-8)^m\right] \\
&\quad + \frac{1}{2^{N}}2\left[\sum_{j=0}^{\frac{N}{2}}\sum_{m=0}^{j}\sum_{l=0}^{N-2m-1}\binom{N}{2j + 1}\binom{j}{m}\binom{N - 2m - 1}{l}e^{ik\cos\hat{\theta}(N-2m-2l-2)}(-8)^m\right] \\
&\quad - \frac{1}{2^{N}}2\left[\sum_{j=0}^{N}\sum_{m=0}^{j}\sum_{l=0}^{N-2m-1}\binom{N}{2j + 1}\binom{j}{m}\binom{N - 2m - 1}{l}e^{ik\cos\hat{\theta}(N-2m-2l)}(-8)^m\right] \\
&= \sum_{l=0}^{N}a_{l,A_1}e^{ik\cos\hat{\theta}(N-2l)}
\end{aligned}
$$

In the last step l is replaced by the variable $l \to l + m$.

$$
\begin{aligned}
p_2^{(N)}(z) &= \frac{1}{2}(1+\frac{z}{\sqrt{z^2-8}})(\frac{z+\sqrt{z^2-8}}{2})^N + \frac{1}{2}(1-\frac{z}{\sqrt{z^2-8}})(\frac{z-\sqrt{z^2-8}}{2})^N \\
&= \frac{1}{2^{N+1}}\left[(1+\frac{z}{\sqrt{z^2-8}})(z+\sqrt{z^2-8})^N + (1-\frac{z}{\sqrt{z^2-8}})(z-\sqrt{z^2-8})^N\right] \\
&= \frac{1}{2^{N+1}}\left[(z+\sqrt{z^2-8})^N + (z-\sqrt{z^2-8})^N + \frac{z}{\sqrt{z^2-8}}\left((z+\sqrt{z^2-8})^N - (z-\sqrt{z^2-8})^N\right)\right] \\
&= \frac{1}{2^{N+1}}\left[\sum_{j=0}^{N}\binom{N}{j}z^{N-j}(\sqrt{z^2-8})^j + \sum_{j=0}^{N}\binom{N}{j}z^{N-j}(-\sqrt{z^2-8})^j\right. \\
&+ \frac{z}{\sqrt{z^2-8}}\left(\sum_{j=0}^{N}\binom{N}{j}z^{N-j}(\sqrt{z^2-8})^j - \sum_{j=0}^{N}\binom{N}{j}z^{N-j}(-\sqrt{z^2-8})^j\right)\Bigg] \\
&= \frac{1}{2^N}\left[\sum_{j=0}^{\frac{N}{2}}\binom{N}{2j}z^{N-2j}(z^2-8)^j + \frac{z}{\sqrt{z^2-8}}\sum_{j=0}^{\frac{N}{2}}\binom{N}{2j+1}z^{N-2j-1}(\sqrt{z^2-8})^{2j+1}\right] \\
&= \frac{1}{2^N}\left[\sum_{j=0}^{\frac{N}{2}}\binom{N}{2j}z^{N-2j}(z^2-8)^j + \sum_{j=0}^{\frac{N}{2}}\binom{N}{2j+1}z^{N-2j}(z^2-8)^j\right] \\
&= \frac{1}{2^N}\left[\sum_{j=0}^{\frac{N}{2}}\binom{N+1}{2j+1}z^{N-2j}(z^2-8)^j\right] \\
&= \frac{1}{2^N}\left[\sum_{j=0}^{\frac{N}{2}}\sum_{m=0}^{j}\binom{N+1}{2j+1}\binom{j}{m}z^{N-2m}(-8)^m\right] \\
&= \frac{1}{2^N}\left[\sum_{j=0}^{\frac{N}{2}}\sum_{m=0}^{j}\sum_{l=0}^{N-2m}\binom{N+1}{2j+1}\binom{j}{m}\binom{N-2m}{l}e^{ik\cos\hat\theta(N-2m-2l)}(-8)^m\right] \\
&= \sum_{l=0}^{N}a_{l,A_2}e^{ik\cos\hat\theta(N-2l)}
\end{aligned}
$$

Derivation of the momentum distribution

$$P(n;T) = \left[|\langle n,1|\psi_\beta(T)\rangle|^2 + |\langle n,2|\psi_\beta(T)\rangle|^2\right]$$

$$= \left[\left|\frac{1}{\sqrt{2\pi}}\int_0^{2\pi} e^{-in\theta}\langle\theta,1|\psi(T)\rangle d\theta\right|^2 + \left|\frac{1}{\sqrt{2\pi}}\int_0^{2\pi} e^{-in\theta}\langle\theta,2|\psi(T)\rangle d\theta\right|^2\right]$$

$$= \left[\left|\frac{1}{\sqrt{2\pi}}\int_0^{2\pi} e^{-in\theta}\langle\theta,1|U_{tot}^T|\psi(0)\rangle d\theta\right|^2 + \left|\frac{1}{\sqrt{2\pi}}\int_0^{2\pi} e^{-in\theta}\langle\theta,2|U_{tot}^T|\psi(0)\rangle d\theta\right|^2\right]$$

$$= \left[\left|\frac{1}{\sqrt{2\pi}}\int_0^{2\pi} e^{-in\theta}\left(\frac{1}{\sqrt{2}}\right)^T \langle\theta,1|\begin{pmatrix} A_1^{(T-1)} & A_2^{(T-1)} \\ A_3^{(T-1)} & A_4^{(T-1)} \end{pmatrix}\right.\right.$$

$$\left.\cdot\frac{1}{\sqrt{2}}(|1\rangle+|2\rangle)\otimes\frac{1}{\sqrt{2}}(|n=0\rangle - i|n=1\rangle)\,d\theta\right|^2$$

$$+\left|\frac{1}{\sqrt{2\pi}}\int_0^{2\pi} e^{-in\theta}\left(\frac{1}{\sqrt{2}}\right)^T \langle\theta,2|\begin{pmatrix} A_1^{(T-1)} & A_2^{(T-1)} \\ A_3^{(T-1)} & A_4^{(T-1)} \end{pmatrix}\right.$$

$$\left.\left.\cdot\frac{1}{\sqrt{2}}(|1\rangle+|2\rangle)\otimes\frac{1}{\sqrt{2}}(|n=0\rangle - i|n=1\rangle)\,d\theta\right|^2\right]$$

$$= \left[\left|\frac{1}{\sqrt{2\pi}}\int_0^{2\pi} e^{-in\theta}\left(\frac{1}{\sqrt{2}}\right)^{T+2}\left(A_1^{(T-1)}+A_2^{(T-1)}\right)(\langle\theta|n=0\rangle - i\langle\theta|n=1\rangle)\,d\theta\right|^2\right.$$

$$\left.+\left|\frac{1}{\sqrt{2\pi}}\int_0^{2\pi} e^{-in\theta}\left(\frac{1}{\sqrt{2}}\right)^{T+2}\left(A_3^{(T-1)}+A_4^{(T-1)}\right)(\langle\theta|n=0\rangle - i\langle\theta|n=1\rangle)\,d\theta\right|^2\right]$$

$$= \frac{1}{2^{T+2}}\left[\left|\frac{1}{\sqrt{2\pi}}\int_0^{2\pi} e^{-in\theta}\left(A_1^{(T-1)}+A_2^{(T-1)}\right)\frac{1}{\sqrt{2\pi}}\left(1-ie^{i\theta}\right)d\theta\right|^2\right.$$

$$\left.+\left|\frac{1}{\sqrt{2\pi}}\int_0^{2\pi} e^{-in\theta}\left(A_3^{(T-1)}+A_4^{(T-1)}\right)\frac{1}{\sqrt{2\pi}}\left(1-ie^{i\theta}\right)d\theta\right|^2\right]$$

$$= \frac{1}{2^{T+2}}\left[\left|\frac{1}{2\pi}\int_0^{2\pi}\left(e^{-in\theta}-ie^{-i(n-1)\theta}\right)\right.\right.$$

$$\left.\cdot\left(\sum_{l=0}^N a_{l,1}e^{ik\cos\hat\theta(N-2l-1)}+i\sum_{l=0}^N a_{l,2}e^{ik\cos\hat\theta(N-2l+1)}\right)d\theta\right|^2$$

$$+\left|\frac{1}{2\pi}\int_0^{2\pi}\left(e^{-in\theta}-ie^{-i(n-1)\theta}\right)\right.$$

$$\left.\left.\cdot\left(\sum_{l=0}^N a_{l,1}e^{-ik\cos\hat\theta(N-2l-1)}+i\sum_{l=0}^N a_{l,2}e^{-ik\cos\hat\theta(N-2l+1)}\right)d\theta\right|^2\right]$$

$$= \frac{1}{2^{T+2}} \left[\left| \sum_{l=0}^{N} a_{l,1} \left[i^{-n} J_{-n}((N-2l-1)k) - i^{-n+2} J_{-n+1}((N-2l-1)k) \right] \right. \right.$$

$$\left. + \sum_{l=0}^{N} a_{l,2} \left[i^{-n+1} J_{-n}((N-2l+1)k) - i^{-n+3} J_{-n+1}((N-2l+1)k) \right] \right|^2$$

$$+ \left| \sum_{l=0}^{N} a_{l,1} \left[i^{-n} J_{-n}(-(N-2l-1)k) - i^{-n+2} J_{-n+1}(-(N-2l-1)k) \right] \right.$$

$$\left. \left. + \sum_{l=0}^{N} a_{l,2} \left[i^{-n+1} J_{-n}(-(N-2l+1)k) - i^{-n+3} J_{-n+1}(-(N-2l+1)k) \right] \right|^2 \right]$$

$$= \frac{1}{2^{T+2}} \left[\left| \sum_{l=0}^{N} a_{l,1} \left[(-1)^n J_n((N-2l-1)k) - i^2 (-1)^{n-1} J_{n-1}((N-2l-1)k) \right] \right. \right.$$

$$\left. + \sum_{l=0}^{N} a_{l,2} \left[i(-1)^n J_n((N-2l+1)k) - i^3 (-1)^{n-1} J_{n-1}((N-2l+1)k) \right] \right|^2$$

$$+ \left| \sum_{l=0}^{N} a_{l,1} \left[(-1)^n J_n(-(N-2l-1)k) - i^2 (-1)^{n-1} J_{n-1}(-(N-2l-1)k) \right] \right.$$

$$\left. \left. + \sum_{l=0}^{N} a_{l,2} \left[i(-1)^n J_n(-(N-2l+1)k) - i^3 (-1)^{n-1} J_{n-1}(-(N-2l+1)k) \right] \right|^2 \right]$$

$$= \frac{1}{2^{T+2}} \left[\left(\sum_{l=0}^{N} a_{l,1} \left[J_n((N-2l-1)k) - J_{n-1}((N-2l-1)k) \right] \right)^2 \right.$$

$$+ \left(\sum_{l=0}^{N} a_{l,2} \left[J_n((N-2l+1)k) - J_{n-1}((N-2l+1)k) \right] \right)^2$$

$$+ \left(\sum_{l=0}^{N} a_{l,1} \left[J_n(-(N-2l-1)k) - J_{n-1}(-(N-2l-1)k) \right] \right)^2$$

$$\left. + \left(\sum_{l=0}^{N} a_{l,2} \left[J_n(-(N-2l+1)k) - J_{n-1}(-(N-2l+1)k) \right] \right)^2 \right]$$

C. Effective Hamiltonian Theory for Harmonic Time Dependence

Often in quantum mechanics we are confronted with Hamiltonian that possess terms whose change is very fast. We define the effective Hamiltonian as the Hamiltonian describing the time averaged time evolution. In this appendix we draft the derivation of a formula to derive the effective Hamiltonian presented in [34].

The time evolution of a quantum mechanical state, in the interaction picture, is given by

$$|\psi(t)\rangle = U(t, t_0)|\psi(t_0)\rangle, \tag{C.1}$$

where $U(t, t_0)$ is the unitary time evolution operator,

$$i\hbar \frac{\partial}{\partial t} U(t, t_0) = H_{\text{int}}(t) U(t, t_0), \tag{C.2}$$

for the interaction Hamiltonian $H_{\text{int}}(t)$.

$\mathcal{H}_{\text{eff}}(t)$ is the effective Hamiltonian, defined in analogy to (C.2) as the Hamiltonian describing the time averaged time evolution. We use that the average of the time derivative is the time derivative of the average.

$$i\hbar \overline{\frac{\partial}{\partial t} U(t, t_0)} = i\hbar \frac{\partial}{\partial t} \overline{U(t, t_0)} = \mathcal{H}_{\text{eff}}(t) \overline{U(t, t_0)} \tag{C.3}$$

By inserting (C.2) into (C.3) we get

$$\mathcal{H}_{\text{eff}}(t) \overline{U(t, t_0)} = \overline{H_{\text{int}}(t) U(t, t_0)}, \tag{C.4}$$

subsequently entailing in

$$\mathcal{H}_{\text{eff}}(t) = \overline{H_{int}(t) U(t, t_0)} \left(\overline{U(t, t_0)} \right)^{-1}. \tag{C.5}$$

Because the time averaging does not preserve the unitarity, $\mathcal{H}_{\text{eff}}$ is not hermitian. One is however only interested in the Hermitian part $\hat{H}_{\text{eff}}(t)$ which is the part describing the unitary

part of the time evolution.

$$H_{\text{eff}}(t) = \frac{1}{2}\left(\mathcal{H}_{\text{eff}}(t) + \mathcal{H}_{\text{eff}}^\dagger(t)\right). \tag{C.6}$$

$\mathcal{H}_{\text{eff}}(t)$ can be computed by using the expansion of the time-ordered time evolution operator:

$$U(t, t_0) = T e^{-\frac{i}{\hbar}\int_{t_0}^t H_{\text{int}}(t')dt'} \tag{C.7}$$

$$= 1 + \underbrace{\frac{1}{i\hbar}\int_{t_0}^t H_{\text{int}}(t')dt'}_{U_1(t)} + \mathcal{O}(H_{\text{int}}^2) \tag{C.8}$$

Here we suppose that the strength of the interaction is weak so that we can stop the expansion before the second order. Inserting (C.8) into (C.5) we get:

$$\mathcal{H}_{\text{eff}}(t) = \overline{H_{\text{int}}(t)} + \overline{H_{\text{int}}(t)U_1(t)} - \overline{H_{\text{int}}(t)}\ \overline{U_1(t)} \tag{C.9}$$

which immediately leads to

$$H_{\text{eff}}(t) = \overline{H_{\text{int}}(t)} + \frac{1}{2}\left(\overline{[H_{\text{int}}(t), U_1(t)]} - \left[\overline{H_{\text{int}}(t)}, \overline{U_1(t)}\right]\right) \tag{C.10}$$

For Hamiltonian with the ensuing harmonic time dependence,

$$H_{\text{int}}(t) = \sum_{n=1}^N \left(h_n e^{-i\omega_n t} + h_n^\dagger e^{i\omega_n t}\right), \tag{C.11}$$

we can easily compute the first order term of U.

$$U_1(t) = V(t) - V(t_0), \tag{C.12}$$

with

$$V(t) = \sum_{n=1}^N \frac{1}{\hbar\omega_n}\left(h_n e^{-i\omega_n t} - h_n^\dagger e^{i\omega_n t}\right). \tag{C.13}$$

$$H_{\text{eff}}(t) = \overline{H_{\text{int}}(t)} + \frac{1}{2}\left(\overline{[H_{\text{int}}(t), V(t)]} - \left[\overline{H_{\text{int}}(t)}, \overline{V(t)}\right]\right) \tag{C.14}$$

where our time averaging procedure is a low pass filter, so that rapidly oscillating terms disappear similar to the rotating wave approximation.

$$\overline{e^{\pm i\omega_n t}} = 0 \tag{C.15}$$

$$\overline{e^{\pm i(\omega_n + \omega_m)t}} = 0 \tag{C.16}$$

$$\overline{e^{\pm i(\omega_n - \omega_m)t}} = e^{\pm i(\omega_n - \omega_m)t} \tag{C.17}$$

From this we get immediately that the following terms vanish:

$$\overline{H_{\text{int}}(t)} = 0 \tag{C.18}$$

$$\overline{V(t)} = 0 \tag{C.19}$$

The final result is:

$$H_{\text{eff}}(t) = \frac{1}{2} \overline{\left[H_{\text{int}}(t), \hat{V}(t) \right]} \tag{C.20}$$

$$= \frac{1}{2} \sum_{m,n=1}^{N} \frac{1}{\hbar \omega_n} \overline{\left[h_m e^{-i\omega_m t} + h_m^\dagger e^{i\omega_m t}, h_n e^{-i\omega_n t} - h_n^\dagger e^{i\omega_n t} \right]} \tag{C.21}$$

$$= \frac{1}{2} \sum_{m,n=1}^{N} \frac{1}{\hbar \omega_n} \overline{[h_m, h_n] e^{-i(\omega_n + \omega_m)t} - \left[h_m, h_n^\dagger \right] e^{i(\omega_n - \omega_m)t}} \tag{C.22}$$

$$\overline{+ \left[h_m^\dagger, h_n \right] e^{i(\omega_m - \omega_n)t} - \left[h_m^\dagger, h_n^\dagger \right] e^{i(\omega_n + \omega_m)t}} \tag{C.23}$$

$$= \frac{1}{2} \sum_{m,n=1}^{N} \frac{1}{\hbar \omega_n} \left(- \left[h_m, h_n^\dagger \right] e^{i(\omega_n - \omega_m)t} + \left[h_m^\dagger, h_n \right] e^{i(\omega_m - \omega_n)t} \right) \tag{C.24}$$

$$= \frac{1}{2} \sum_{m,n=1}^{N} \left(\frac{1}{\hbar \omega_m} \left[h_m^\dagger, h_n \right] e^{i(\omega_m - \omega_n)t} + \frac{1}{\hbar \omega_n} \left[h_m^\dagger, h_n \right] e^{i(\omega_m - \omega_n)t} \right) \tag{C.25}$$

$$= \sum_{m,n=1}^{N} \frac{1}{\hbar \bar{\omega}_{mn}} \left[h_m^\dagger, h_n \right] e^{i(\omega_m - \omega_n)t} \tag{C.26}$$

where $\bar{\omega}_{mn}$ is

$$\bar{\omega}_{mn} = \frac{2}{\left(\frac{1}{\omega_m} + \frac{1}{\omega_n} \right)}, \tag{C.27}$$

the harmonic average between ω_m and ω_n.

D. More figures on the influence of the kick strength
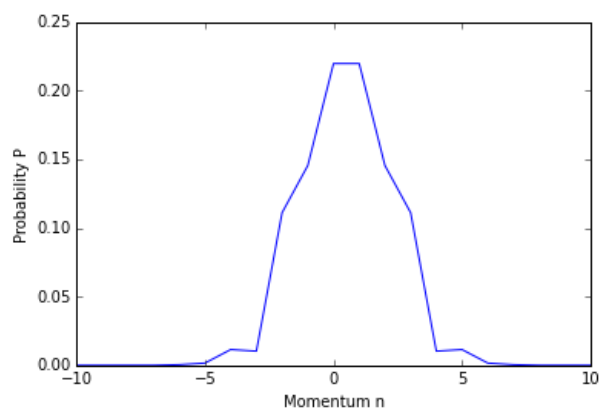
$k = 0.5$
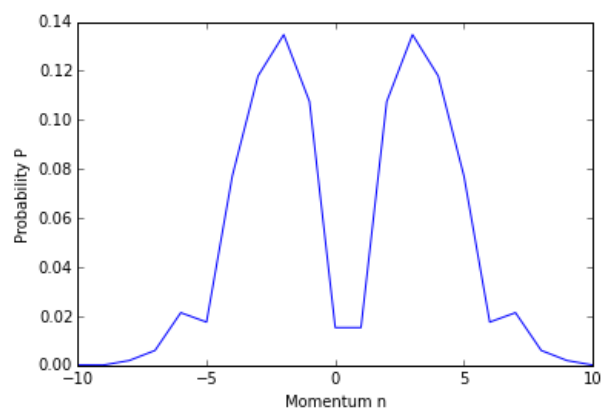
$k = 0.75$
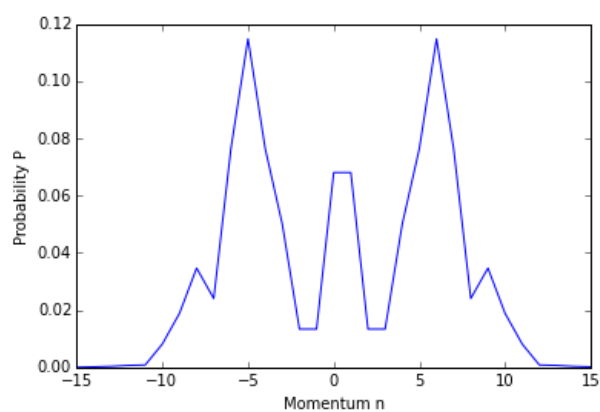
$k = 1$
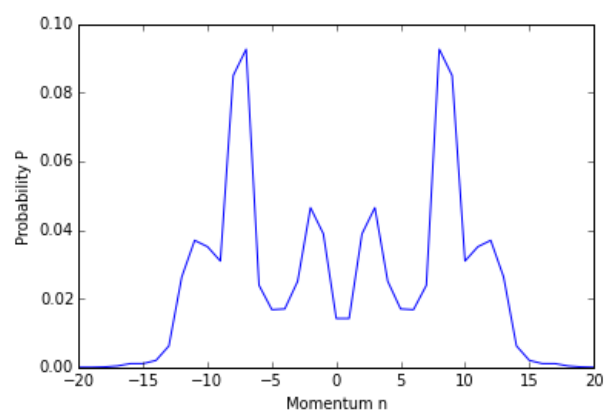
$k = 1.25$
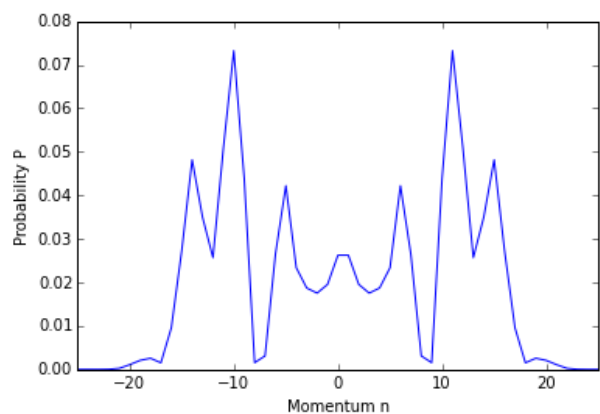
$k = 1.5$
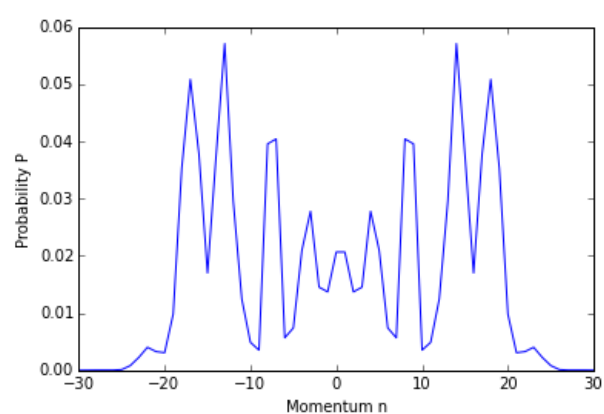
$k = 1.75$
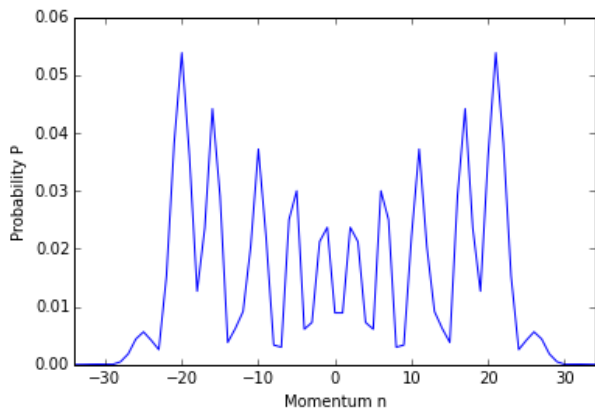
$k = 2$
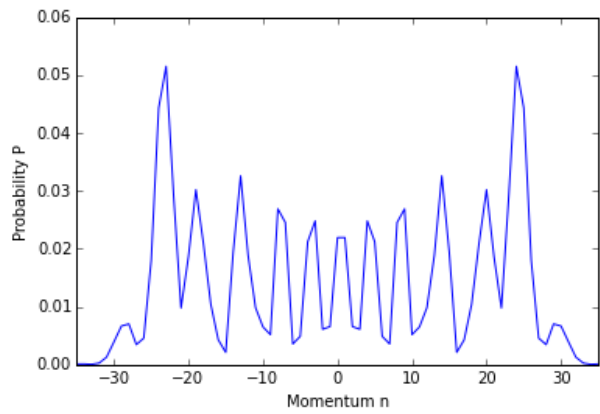
$k = 2.25$
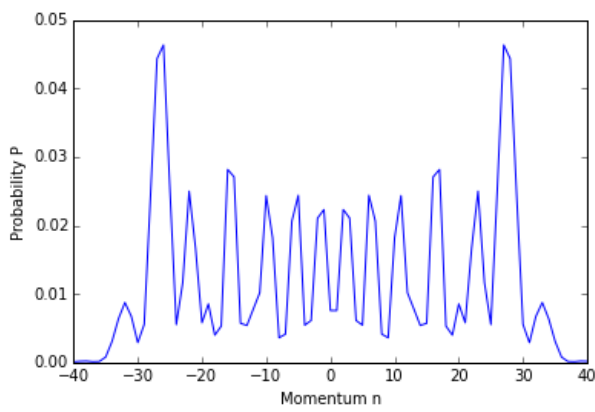
$k = 2.5$
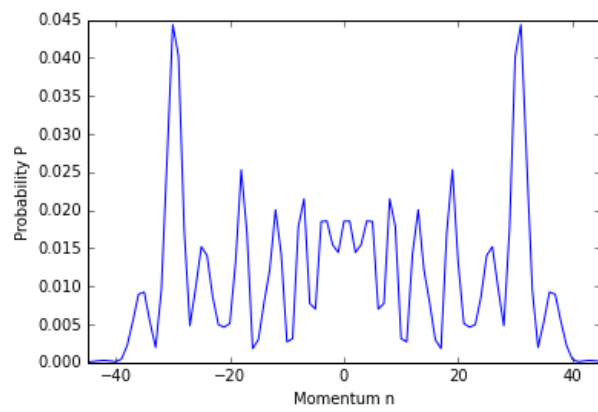
$k = 2.75$
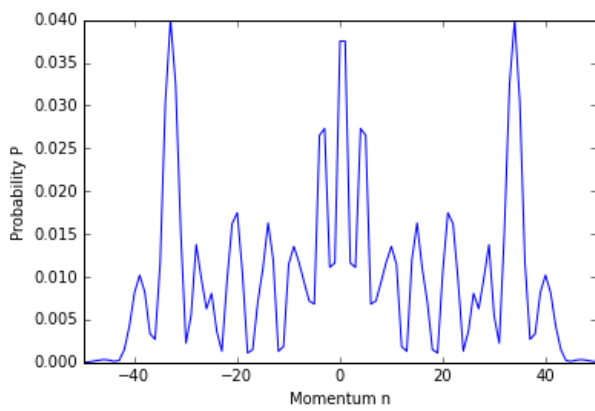
$k = 3$
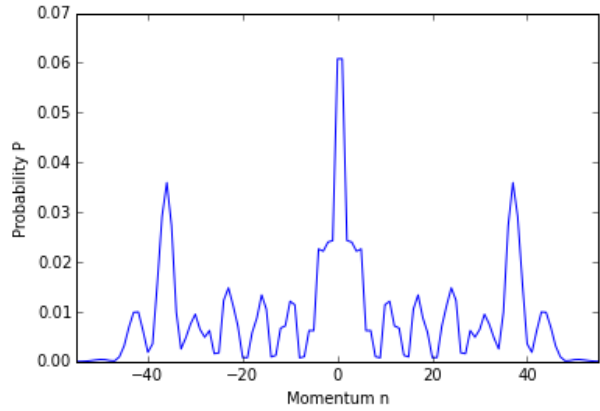
$k = 3.25$
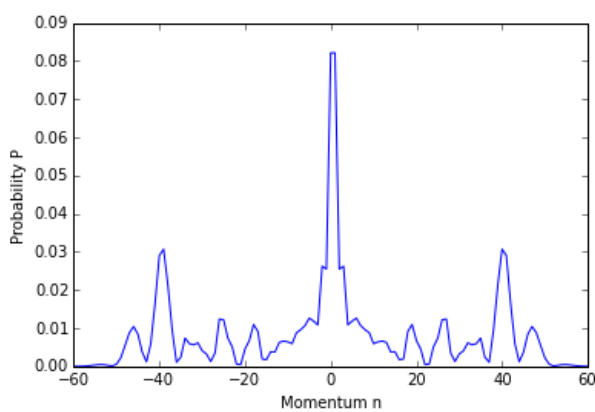
$k = 3.5$
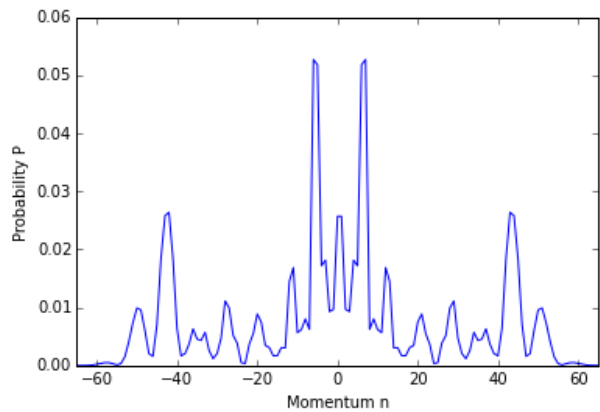
$k = 3.75$
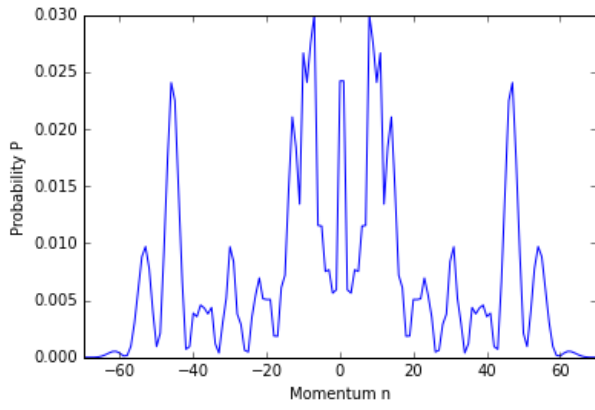
$k = 4$
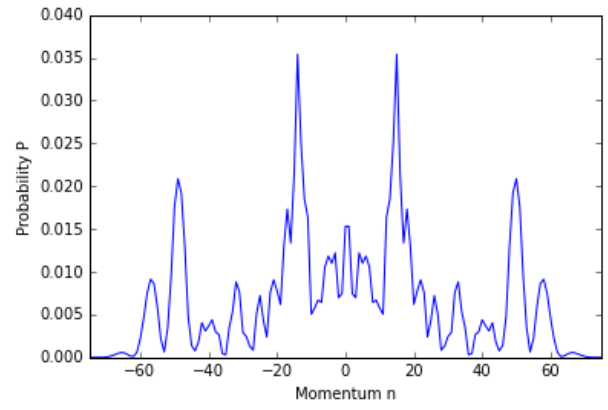
$k = 4.25$
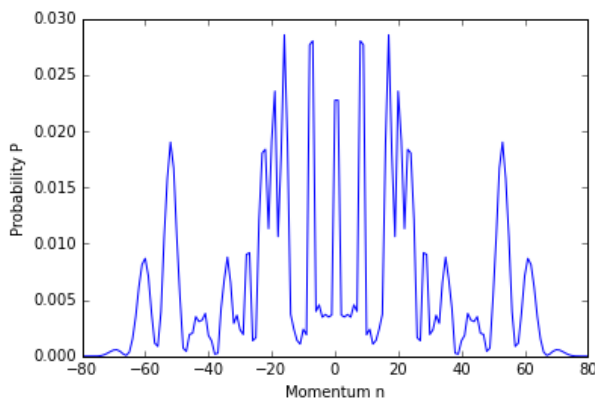
$k = 4.5$
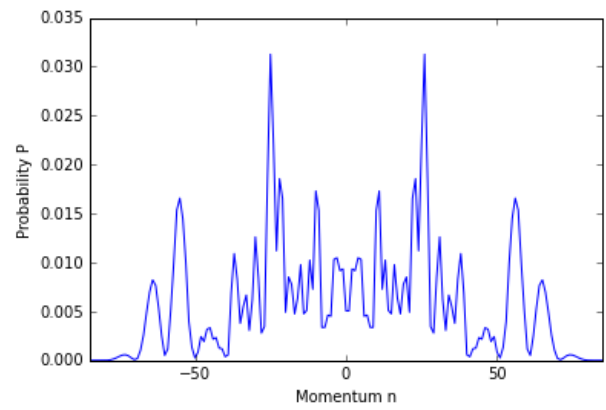
$k = 4.75$
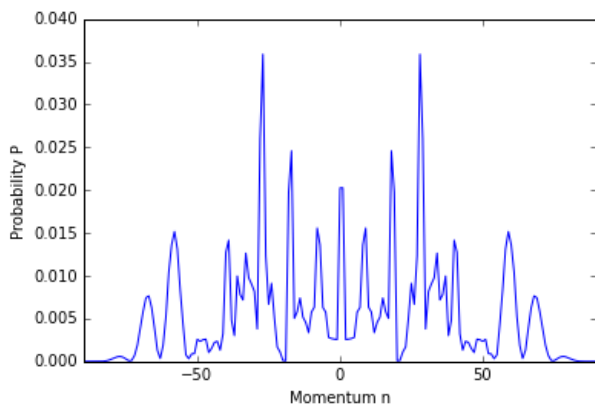
$k = 5$
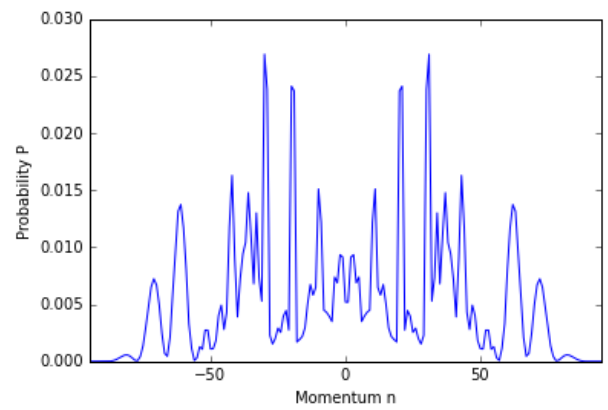
$k = 5.25$
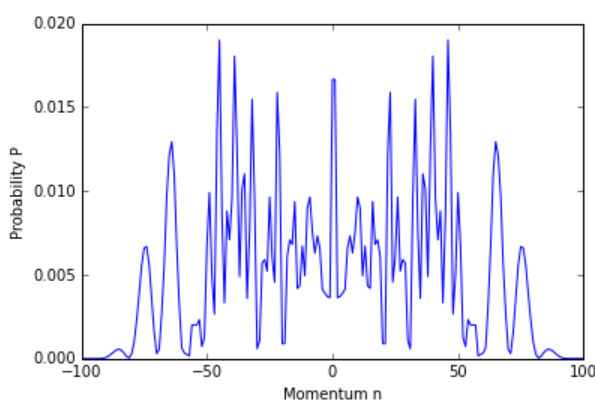
$k = 5.5$
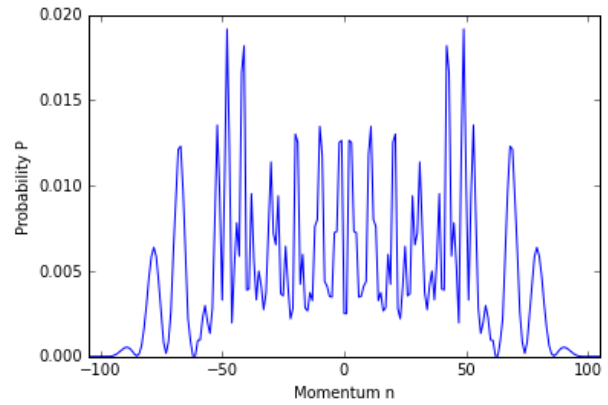
$k = 5.75$

$k = 6$ $k = 6.25$

List of Figures

Bibliography

[1] M. A. Nielsen and I. L. Chuang, *Quantum Computation and Quantum Information*. 10th Anniversary Edition, Cambridge University Press (2010).

[2] Y. Aharonov, L. Davidovich and N. Zagury, *Quantum random walks*. Phys. Rev. A 48, 1687 (1993).

[3] J. Kempe, *Quantum Random Walks Hit Exponentially Faster*. arXiv:quant-ph/0205083.

[4] A. M. Childs, *Universal Computation by Quantum Walk*. Phys. Rev. Lett. 102, 180501 (2009).

[5] A. Schreiber, K. N. Cassemiro, V. Potocek, A. Gábris, P. J. Mosley, E. Andersson, I. Jex, and C. Silberhorn , *Photons Walking the Line: A Quantum Walk with Adjustable Coin Operations*. Phys. Rev. Lett. 104, 050502 (2010).

[6] M. Karski, L. Förster, J. Choi, A. Steffen, W. Alt, D. Meschede and A. Widera, *Quantum Walk in Position Space with Single Optically Trapped Atoms*. Science 325, 174 (2009).

[7] G. S. Summy and S. Wimberger, *Quantum random walk of a Bose-Einstein condensate in momentum space*. Phys. Rev. A 93, 023638 (2016).

[8] B. V. Chirikov, *Research concerning the theory of nonlinear resonance and stochasticity*. Preprint N 267, Institute of Nuclear Physics, Novosibirsk (1969).

[9] F. Izrailev, *Simple models of quantum chaos: spectrum and eigenfunctions*. Phys. Rep. 196, 299 (1990).

[10] M. G. Raizen, F. L. Moore, J. C. Robinson, C. F. Bharucha and B. Sundaram, *An experimental realization of the quantum δ-kicked rotor*. Quantum Semiclass. Opt. 8: Journal of the European Optical Society Part B, pages 687-692 (1996).

[11] D. H. White, S. K. Ruddell, and M. D. Hoogerland, *Experimental realization of a quantum ratchet through phase modulation*. Phys. Rev. A 88, 063603 (2013).

[12] R. K. Shrestha, S. Wimberger, J. Ni, W. K. Lam and G. S. Summy, *Fidelity of the quantum δ-kicked accelerator*. Phys. Rev. E 87, 020902 (2013).

[13] S. Wayper, M. Sadgrove, W. Simpson and M. Hoogerland, *Atom optics kicked rotor: experimental evidence for a pendulum description of the quantum resonance*. arXiv:quant-ph/0504219v1.

[14] M. Sadgrove and S. Wimberger, *A Pseudoclassical Method for the Atom-Optics Kicked Rotor: from Theory to Experiment and Back.* Adv. At. Mol. Phys. 60, 315 (2011).

[15] F. L. Moore, J. C. Robinson, C. F. Bharucha, P. E. Williams and M. G. Raizen, *Observation of dynamical localization in atomic momentum transfer: a new testing ground for quantum chaos.* Phys. Rev. Lett. 73, 2974 (1994).

[16] I. Guarneri, L. Rebuzzini, and S. Fishman, *A Theory for Quantum Accelerator Modes in Atom Optics.* Journal of Statistical Physics 110, 911 (2003).

[17] D. A. Steck, *Quantum Chaos, Transport, and Decoherence in Atom Optics.* Doctor of Philosophy thesis, University of Texas, Austin (2001).

[18] S. Wimberger, I. Guarneri and S. Fishman, *Quantum resonances and decoherence for delta-kicked atoms.* Nonlinearity 16, 1381 (2003).

[19] R. Feynman, *Lectures on Physics I.* Addison-Wesley, chapter 46 (1963).

[20] R. D. Astumian and P. Hänggi, *Brownian Motors.* Physics Today 55, 33 (2002).

[21] R. D. Astumian and M. Bier, *Mechanochemical Coupling of the Motion of Molecular Motors to ATP Hydrolysis.* Biophysical Journal 70, 637 (1996).

[22] A. M. Ishkhanyan, *Narrowing of interference fringes in diffraction of prepared atoms by standing waves.* Phys. Rev. A 61, 063609 (2000).

[23] A. M. Ishkhanyan, *Diffraction of atoms by a standing wave at Gaussian initial momentum distribution of amplitudes.* Phys. Rev. A 61, 063611 (2000).

[24] J. Ni, W. K. Lam, S. Dadras, M. F. Borunda, S. Wimberger and G. S. Summy, *Initial-state dependence of a quantum resonance ratchet.* Phys Rev. A 94, 043620 (2016).

[25] J. Ni, W. K. Lam, R. K. Shrestha, M. Sadgrove, S. Wimberger and G. S. Summy, *Hamiltonian Ratchets with Ultra-Cold Atoms.* Ann. Phys. (Berlin), 1600335 (2017).

[26] J. Kempe, *Quantum random walks - an introductory overview.* Contemp. Phys. 44, 307 (2003).

[27] V. Kendon and B. Tregenna, *Decoherence can be useful in quantum walks.* Phys. Rev. A 67, 042315 (2003).

[28] S. Wimberger, *Nonlinear Dynamics and Quantum Chaos - An Introduction.* Springer, (2014).

[29] W. H. Press, S. A. Teukolsky, W. T. Vetterling and B. P. Flannery, *Numerical Recipes - The Art of Scientific Computing, Third Edition.* Cambridge University Press, New York (2007).

[30] K. Mølmer, Y. Castin and J. Dalibard, *Monte Carlo wave-function method in quantum optics.* J. Opt. Soc. Am. B 10, 524 (1993).

[31] M. B. d'Arcy, *Quantum chaos in atom optics.* Ph.D. thesis, University of Oxford (2002).

[32] D. A. Steck, *Quantum Chaos, Transport, and Decoherence in Atom Optics.* Ph.D. thesis, University of Texas, Austin (2001).

[33] M. Alexanian and S. K. Bose, *Unitary transformation and the dynamics of a three-level atom interacting with two quantized field modes.* Phys. Rev. A 52, 023638 (1995).

[34] D. F. V. James and J. Jerke, *Effective Hamiltonian theory and its applications in quantum information.* Can. J. Phys. 85, 625 (2007).

[35] D. Steck, *Rubidium 87 D Line Data.* http://steck.us/alkalidata/.

[36] S. Wimberger, *Chaos and Localisation: Quantum Transport in Periodically Driven Atomic Systems.* Ph.D. Thesis, University of Munich and University of Insubria (2004).

[37] C. Ryu, M. F. Andersen, A. Vaziri, M. B. d'Arcy, J. M. Grossman, K. Helmerson, W. D. Phillips, *High-order quantum resonances observed in a periodically kicked bose-einstein condensate.* Phys. Rev. Lett. 96, 160403 (2006).

[38] Courtesy of G. S. Summy.

[39] H. P. Breuer and F. Petruccione, *The Theory of open quantum systems.* Oxford University Press (2002).

[40] R. K. Shrestha, J. Ni, W. K. Lam, G. S. Summy and S. Wimberger, *Dynamical tunneling of a Bose-Einstein condensate in periodically driven systems.* Phys. Rev. E 88, 034901 (2013).

[41] H. Yokoyama and K. Ujihara, *Spontaneous Emission and Laser Oscillations in Microcavities.* CRC Press (1995).

[42] M. Wilkens, *Significance of Röntgen current in quantum optics: Spontaneous emission of moving atoms.* Phys. Rev. A 49, 570 (1994).

[43] V.K. Rohatgi, *An Introduction to Probability Theory Mathematical Statistics.* Wiley, (1976).

[44] F. Reiter and A. S. Sørensen, *Effective operator formalism for open quantum systems.* Phys. Rev. A 85, 032111 (2012).

[45] A. Vukics, *Of quantum mechanical pictures.* http://optics.szfki.kfki.hu/Vukics/Vukics.

[46] A. C. Doherty, K. M. D. Vant, G. H. Ball, N. Christensen and R. Leonhardt, *Momentum distributions for the quantum δ-kicked rotor with decoherence.* J. Opt. B: Quantum Semiclass. Opt. 2, 605 (2000).

[47] S. Dyrting, *Modifications to the chaotic dynamics of laser-cooled atoms due to spontaneous emission.* Phys. Rev. A 53, 2522 (1996).

[48] M. Weiß, C. Groiseau, W. K. Lam, R. Burioni, A. Vezzani, G. S. Summy and S. Wimberger, *Steering random walks with kicked ultracold atoms.* Phys. Rev. A 92, 033606 (2015).

[49] A. Schreiber, K. N. Cassemiro, V. Potocek, A. Gábris, I. Jex and C. Silberhorn, *Decoherence and Disorder in Quantum Walks: From Ballistic Spread to Localization.* Phys. Rev. Lett. 106, 180403 (2011).

[50] M. Abramowitz and I. A. Stegun, *Handbook of Mathematical Functions with Formulas, Graphs, and Mathematical Tables.* United States Department of Commerce, National Bureau of Standards (1964).

Erklärung

Ich versichere, dass ich diese Arbeit selbstständig verfasst und keine anderen als die angegebenen Quellen und Hilfsmittel benutzt habe.

Heidelberg, den 20. Juli 2017,